EUROPEAN ORGANIZATION FOR NUCLEAR RESEARCH (CERN)

CERN-EP-2024-251
2024/11/07

CMS-TOP-23-004

Measurements of inclusive and differential cross sections for top quark production in association with a Z boson in proton-proton collisions at $\sqrt{s} = 13\,\text{TeV}$

The CMS Collaboration*

Abstract

Measurements are presented of inclusive and differential cross sections for Z boson associated production of top quark pairs ($\mathrm{t\bar{t}Z}$) and single top quarks (tZq or tWZ). The data were recorded in proton-proton collisions at a center-of-mass energy of 13 TeV, corresponding to an integrated luminosity of $138\,\text{fb}^{-1}$. Events with three or more leptons, electrons or muons, are selected and a multiclass deep neural network is used to separate three event categories, the $\mathrm{t\bar{t}Z}$ and tWZ processes, the tZq process, and the backgrounds. A profile likelihood approach is used to unfold the differential cross sections, to account for systematic uncertainties, and to determine the correlations between the two signal categories in one global fit. The inclusive cross sections for a dilepton invariant mass between 70 and 110 GeV are measured to be $1.14 \pm 0.07\,\text{pb}$ for the sum of $\mathrm{t\bar{t}Z}$ and tWZ, and $0.81 \pm 0.10\,\text{pb}$ for tZq, in good agreement with theoretical predictions.

Submitted to the Journal of High Energy Physics

*See Appendix A for the list of collaboration members

1 Introduction

At the CERN LHC, precise inclusive and differential measurements of top quark production in association with a Z boson have made it possible to directly probe the couplings between the top quark and the Z boson. Possible physics beyond the standard model (SM) of particle physics could induce measurable deviations from SM expectations, as described, e.g., in Ref. [1]. Furthermore, processes involving top quarks and Z bosons are significant backgrounds to other important SM processes, such as Higgs boson production in association with a top quark [2]. These measurements also allow for tests of theory calculations in perturbative quantum chromodynamics (pQCD) and studies of the modeling in Monte Carlo (MC) generators.

Measurements of Z boson production in association with top quark pairs ($\mathrm{t\bar{t}Z}$) and single top quarks with an additional light-flavor quark q (tZq) have been performed by the ATLAS [3–9] and CMS [10–15] experiments. The cross sections for $\mathrm{t\bar{t}Z}$ and tZq are expected to be of similar order of magnitude, despite their different orders in the strong coupling α_S [16]. Generally good agreement with the SM expectations was found [2, 17–20]. The CMS Collaboration recently reported the first evidence for single top quark production in association with both a W and a Z boson (tWZ) [21]. The inclusive tWZ cross section was measured to be $\sigma_{\mathrm{tWZ}} = 354 \pm 54\,\mathrm{(stat)} \pm 95\,\mathrm{(syst)}$ fb, about two standard deviations above the SM expectation of $136\,^{+9}_{-8}$ fb [22].

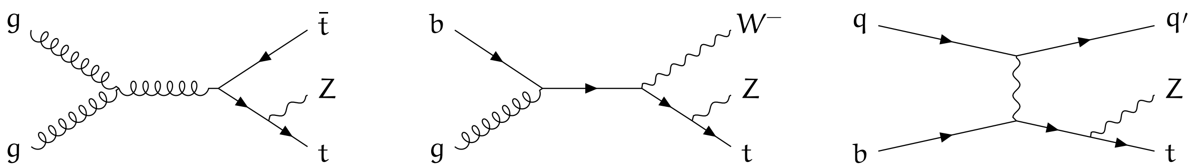

Figure 1: Leading order Feynman diagrams for the $\mathrm{t\bar{t}Z}$ (left), tWZ (middle), and tZq (right) processes.

Leading order (LO) Feynman diagrams for the processes $\mathrm{t\bar{t}Z}$, tWZ, and tZq are shown in Fig. 1. Experimentally, the Z boson is reconstructed in its leptonic decays into a pair of leptons (electrons or muons, in the following collectively denoted by the ℓ symbol). For signal events with three leptons in the final state, at LO, the three signal processes differ in the jet multiplicity distributions. For $\mathrm{t\bar{t}Z}$, in which the $\mathrm{t\bar{t}}$ system decays in the lepton+jets channel, four central jets are expected of which two originate from b quarks. For tWZ, three central jets including one b jet are expected. For tZq, there is one b jet and one light quark jet, and the light-flavor recoil jet often has a high absolute pseudorapidity $|\eta|$ and transverse momentum p_{T}. Higher-order effects and limitations in detector acceptance lead to a large overlap between the measured jet multiplicity distributions. In addition, at next-to-leading order (NLO) in pQCD, interference terms between $\mathrm{t\bar{t}Z}$ and tWZ appear [23], making the individual measurements more difficult. Therefore, in this analysis, the two processes $\mathrm{t\bar{t}Z}$ and tWZ are measured together.

In this paper, the cross sections for single and pair production of top quarks in association with a Z boson are simultaneously measured for the first time. Both inclusive and differential measurements are reported for $\mathrm{t\bar{t}Z}$+tWZ and tZq. In previous publications, separate analyses for the $\mathrm{t\bar{t}Z}$ and tZq processes were reported, assuming SM expectations for one process while measuring the other. In the simultaneous analysis presented here, information about the correlation between the processes is obtained directly. This information can be useful, e.g., in global fits using effective field theory (EFT) [24, 25] in which the combined sensitivity of data from different measurements can be used to obtain optimal constraints [26, 27].

The analysis makes use of proton-proton (pp) collision data recorded at the CMS experiment in the years 2016–2018 at a center-of-mass energy of 13 TeV, corresponding to an integrated luminosity of $138\,\mathrm{fb}^{-1}$. For the differential measurement, events are selected with exactly three isolated leptons, of which two originate from the Z boson, while the third comes from the decay of a W boson. For the inclusive measurement, events with four leptons are also included, as described in more detail in Section 6. In the cases of $\mathrm{t\bar{t}Z}$ and tZq, the W boson originates from the top quark decay, while in the tWZ process it can also be produced directly. A multiclass deep neural network (DNN) is used to determine event likelihood scores for each of the three categories: 1) the signal category $\mathrm{t\bar{t}Z}$+tWZ, used to measure the combined cross section of $\mathrm{t\bar{t}Z}$ and tWZ; 2) the tZq signal category; and 3) the background category. An important background process is WZ production. Another background, referred to as "nonprompt leptons", arises in processes with large cross sections, such as Z+jets and inclusive $\mathrm{t\bar{t}}$ production, if particles not originating from the decay of a real vector boson mimick the signature of leptons in the detector. In the fit, a given event is assigned to the category with the highest score. Both inclusive and differential cross sections for the two signal processes are measured simultaneously using a profile likelihood fit approach, in which nuisance parameters are implemented to constrain the systematic uncertainties, and the free parameters of interest are determined simultaneously, for each signal process and in each bin of the measurement, together with their correlation matrix.

The paper is structured as follows. In Section 2, an overview of the CMS detector is given. Subsequently, in Section 3, the data and MC simulation samples are described. The event selection, the resulting composition of signal and background events and their classification into two signal categories and the background are presented in Section 4. The systematic uncertainties and the results of the measurement are reported in Sections 5 and 6. Finally, a summary is given in Section 7. Tabulated results can be found in HEPData [28].

2 The CMS detector and event reconstruction

The central feature of the CMS apparatus is a superconducting solenoid of 6 m internal diameter, providing a magnetic field of 3.8 T. Within the solenoid volume are a silicon pixel and strip tracker, a lead tungstate crystal electromagnetic calorimeter (ECAL), and a brass and scintillator hadron calorimeter (HCAL), each composed of a barrel and two endcap sections. Forward calorimeters extend the pseudorapidity coverage provided by the barrel and endcap detectors. Muons are measured in gas-ionization detectors embedded in the steel flux-return yoke outside the solenoid. A more detailed description of the CMS detector, together with a definition of the coordinate system used and the relevant kinematic variables, can be found in Refs. [29, 30].

The particle-flow (PF) event reconstruction [31] aims to reconstruct and identify each individual particle in an event, with an optimized combination of information from all CMS detector components. In the PF algorithm, the identification of the particle type (photon, electron, muon, charged or neutral hadron) plays an important role in the determination of the particle direction and energy. The primary vertex is taken to be the vertex corresponding to the hardest scattering in the event, evaluated using tracking information alone, as described in Section 9.4.1 of Ref. [32].

The electron momentum is estimated by combining the energy measurement in the ECAL with the momentum measurement in the tracker. Muons are identified as tracks in the central tracker consistent with either a track or several hits in the muon system, and associated with calorimeter deposits compatible with the muon hypothesis. Charged hadrons are identified as charged-particle tracks that are neither identified as electrons nor as muons. The energy of charged hadrons is determined from a combination of the track momentum and the corresponding ECAL and HCAL energies, corrected for the response function of the calorimeters to hadronic showers. Neutral hadrons are identified as HCAL energy clusters not linked to any charged-hadron trajectory, or as a combined ECAL and HCAL energy excess with respect to the expected charged-hadron energy deposit. The energy of neutral hadrons is obtained from the corresponding corrected ECAL and HCAL energies.

For each event, hadronic jets are clustered from these reconstructed particles using the anti-k_{T} algorithm [33, 34] with a distance parameter of 0.4. Additional pp interactions within the same or nearby bunch crossings (pileup) can contribute additional tracks and calorimetric energy deposits to the jet momentum. To mitigate this effect, charged particles identified as originating from pileup vertices are discarded and an offset correction is applied to correct for the remaining contributions [35]. Jet energy corrections (JEC) are derived from simulation studies so that the average measured energy of jets becomes identical to that of particle level jets, and residual differences between data and simulation are determined using momentum balance measurements in dijet, photon+jet, Z+jet, and multijet events [36].

To identify (tag) jets originating from b quarks (b jets), information about the energy of particles, tracks, and vertices inside the jet is fed into the DEEPJET DNN [37]. A b tagging requirement is applied in this analysis by using a minimum threshold on the b tagging score, corresponding to a 75% efficiency (1% mistagging rate) for b jets (light jets). This reconstruction method is applied only for jets within the acceptance of the silicon tracker ($|\eta| < 2.4$ for 2016 and $|\eta| < 2.5$ for 2017–2018).

The missing transverse momentum vector $\vec{p}_{\mathrm{T}}^{\text{miss}}$ is computed as the negative vector p_{T} sum of all the PF candidates in an event, and its magnitude is denoted as $p_{\mathrm{T}}^{\text{miss}}$ [38]. The $\vec{p}_{\mathrm{T}}^{\text{miss}}$ is modified to account for corrections to the energy scale of the reconstructed jets in the event.

3 Event simulation

The MC simulation samples for the signal processes (tZq, $\mathrm{t\bar{t}Z}$, and tWZ), are generated at NLO with MADGRAPH5_aMC@NLO v2.6.5 [22]. The same generator is used for the production of a W boson and a Z boson (WZ), the $\mathrm{t\bar{t}}$ production in association with a W boson ($\mathrm{t\bar{t}W}$), the production of three electroweak gauge bosons, and the production of a photon in association with a W or Z boson ($\mathrm{V}\gamma$). Other backgrounds, such as $\mathrm{t\bar{t}}$ production in association with a photon or with two electroweak gauge bosons, are simulated with MADGRAPH5_aMC@NLO at LO accuracy. Some minor backgrounds, e.g., $\mathrm{t\bar{t}}$ production in association with a Higgs boson ($\mathrm{t\bar{t}H}$) and the quark-initiated production of two Z bosons (ZZ), are simulated at NLO accuracy in pQCD using POWHEG v2 [39], while the gluon-initiated ZZ production is simulated at LO with the MCFM v7.0.1 [40] generator. In the following, backgrounds arising from $\mathrm{t\bar{t}W}$, $\mathrm{t\bar{t}H}$, as well as from $\mathrm{t\bar{t}}$ production in association with a photon or with two vector bosons, are referred to as $\mathrm{t\bar{t}X}$, the production of two or three heavy bosons, excluding WZ production, is referred to as multiboson production.

The generators are interfaced with the parton shower program PYTHIA v8.240 [41] using the CP5 underlying event tune [42]. To avoid double-counting between the matrix element generation with MADGRAPH5_aMC@NLO and the parton shower, the FxFx [43] (MLM [44]) jet matching schemes are used for simulations at NLO (LO). For the tZq sample, the four-flavor scheme (4FS) is used. In the 4FS, the b quark in the initial state originates from gluon splitting at the matrix element level. The 4FS is expected to provide a better modeling of the event kinematics than the five-flavor scheme (5FS) [20], which is employed for all other samples. In the 5FS, the b quark comes directly from the parton distribution function (PDF), and the total cross section prediction is expected to be more precise [20]. The samples are simulated with the NNPDF v3.1 [45] PDF set at NLO accuracy.

At NLO, tWZ production interferes with the LO $\mathrm{t\bar{t}Z}$ process. The diagram removal (DR) and diagram subtraction (DS) approaches are used to remove the double counting. In the DR scheme, the overlap is removed at the amplitude level, either excluding (DR1) or including (DR2) the interference term [46, 47]. In the DS scheme, the overlap is removed at the cross section level. In this analysis, the nominal tWZ event samples are generated using the DR1 method, and alternative samples, produced with the DR2 method, are used to estimate the corresponding uncertainty. As reported in Ref. [47], the result of the DS scheme lies between DR1 and DR2, and it is thus not included as an uncertainty in this measurement.

The CMS detector response is simulated using GEANT4 [48]. The effect of additional pp interactions within the same or nearby bunch crossings (pileup) is taken into account by adding simulated minimum-bias interactions to the simulated data.

4 Event selection and background estimation

The event selection criteria are designed to efficiently select tZq, $\mathrm{t\bar{t}Z}$, and tWZ signal events while suppressing the background. Events are selected if they contain three or more leptons, which are reconstructed within $|\eta| < 2.5$ for electrons and $|\eta| < 2.4$ for muons. The three leptons, when ordered in decreasing p_{T}, are required to have $p_{\mathrm{T}} > 25$, 15, and 10 GeV. Two of the leptons must be of the same flavor and opposite charge, and have an invariant mass between 70 and 110 GeV; the third one is expected to originate from the W boson. A combination of trigger algorithms requiring the presence of either one, two, or three leptons is used to record the events.

To suppress backgrounds, selected leptons are required to fulfill additional "tight" selection requirements based on a multivariate classifier [14, 15, 49], which distinguishes prompt leptons that are created in the decay of a W or Z boson from nonprompt leptons. The prompt-lepton selection efficiencies in the simulation are corrected to match those in the data using scale factors (SFs) which are evaluated using a "tag-and-probe" method in $\mathrm{Z} \to \ell^+\ell^-$ events [50, 51].

Jets are required to have $p_{\mathrm{T}} > 25$ GeV and $|\eta| < 5.0$ and to be separated in space from each lepton by $\Delta R = \sqrt{(\Delta\eta)^2 + (\Delta\phi)^2} > 0.4$, where $\Delta\eta$ and $\Delta\phi$ are the differences in η and azimuthal angle, respectively, between the jet and the lepton. At least two jets, of which at least one must be b tagged, are also required in each event.

Dominant contributions to the nonprompt background come from $\mathrm{t\bar{t}}$ and Drell–Yan production where two genuine prompt leptons are expected; the third lepton candidate then often comes from a decay of a hadron. The nonprompt-lepton background contribution is estimated from data, separately for electrons and muons, following an approach similar to that described in Ref. [15]. In this approach, a lepton misidentification rate is determined from simulated QCD multijet samples. This information is then used to determine a transfer factor that is applied to events in data that are selected similarly to those in the signal region, but with looser lepton requirements. The obtained distribution describes the expectation for the nonprompt background in the signal region.

Figures 2 and 3 show comparisons of measured and expected distributions of the events that fulfill the signal selection criteria. In Fig. 2, the transverse momenta of the leptons with the highest and second highest p_{T} are presented, the jet and b jet multiplicities, and the $|\eta|$ of the

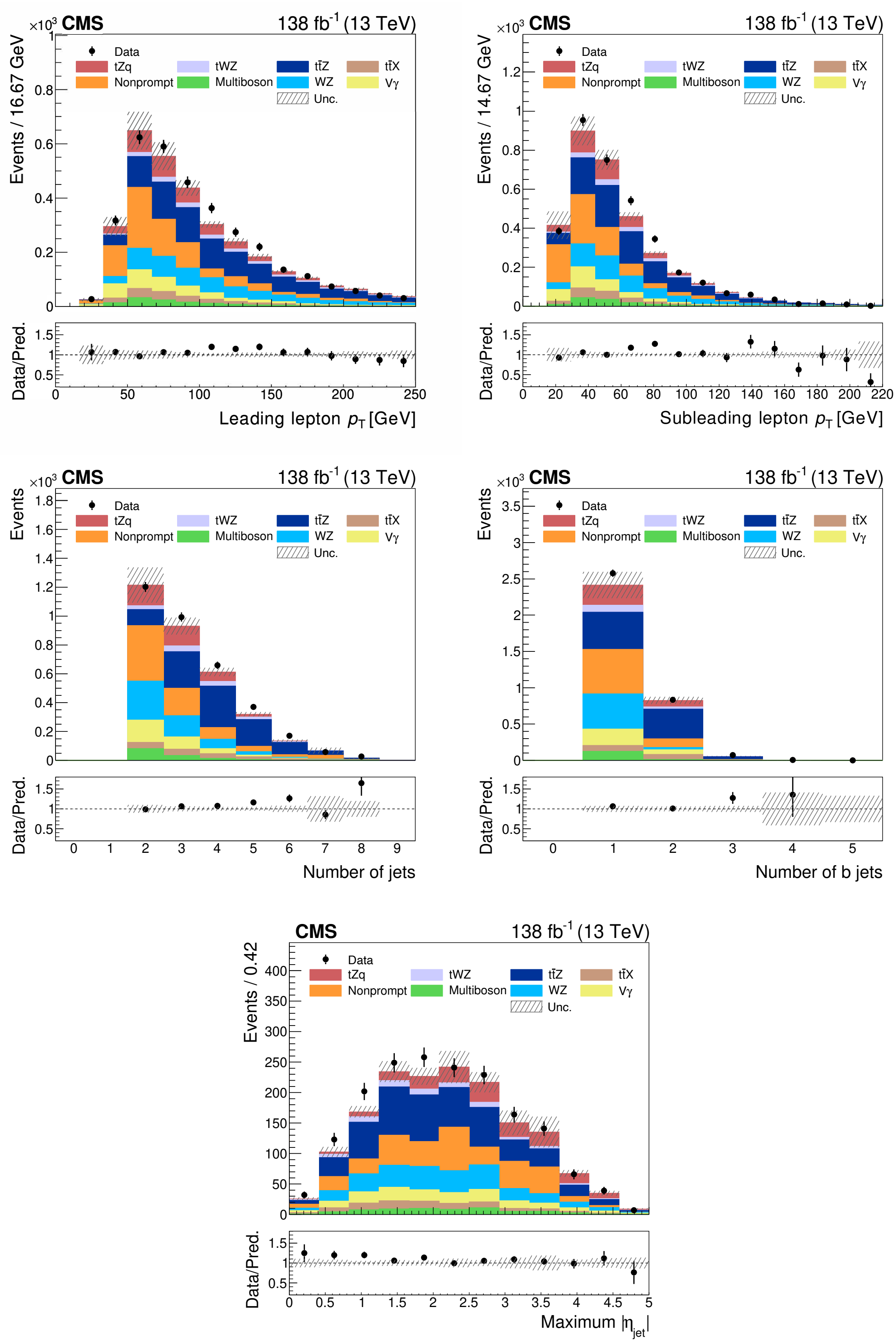

Figure 2: Distributions after final event selection: the p_{T} of the lepton with the highest (upper left) and second highest (upper right) p_{T}, the number of jets (middle left), the number of b jets (middle right), and the $|\eta|$ of the jet with the highest $|\eta|$ (lower). The data are displayed as points with statistical error bars and the expectation is shown with a histogram with the systematic uncertainty given by the hatched area.

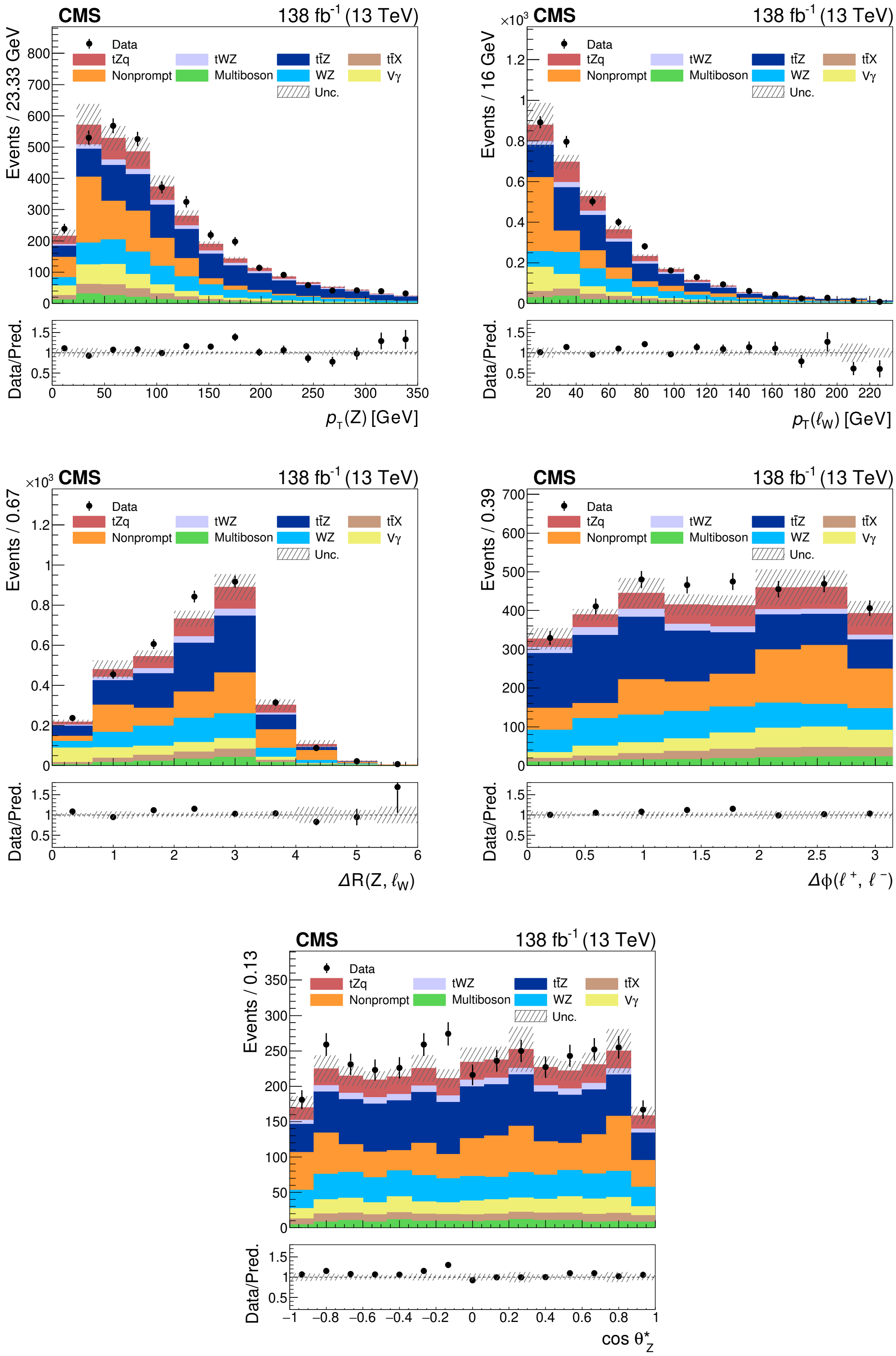

Figure 3: Distributions after final event selection: the p_T of the reconstructed Z boson (upper left), the p_T of the lepton arising from the W boson $p_T(\ell_W)$ (upper right), $\Delta R(Z, \ell_W)$ (middle left), $\Delta\phi(\ell^+, \ell^-)$ (middle right), and the cosine of the angle $\cos\theta^*_Z$ between the Z boson and its negatively charged decay lepton in the Z boson rest frame (lower). The data are displayed as points with statistical error bars and the expectation is shown with a histogram with the systematic uncertainty given by the hatched area.

highest-$|\eta|$ jet. Figure 3 shows distributions of the p_{T} of the reconstructed Z boson, the p_{T} of the lepton originating from the W boson $p_{\mathrm{T}}(\ell_{\mathrm{W}})$, the separation $\Delta R(\mathrm{Z}, \ell_{\mathrm{W}})$ between the Z boson and the lepton originating from the W boson decay, the azimuthal angle $\Delta\phi(\ell^{+}, \ell^{-})$ between the two leptons originating from the Z boson decay in the lab frame, and the cosine of the angle $\cos\theta^{*}_{\mathrm{Z}}$ between the Z boson and its negatively charged decay lepton in the Z boson rest frame. These are the observables for which the differential cross sections are reported in Section 6.2.

The Z boson candidate is reconstructed from the opposite-sign same-flavor lepton pair with the closest invariant mass to that of the Z boson. The third lepton is then interpreted as originating from the W boson. Reasonable agreement can be seen between the expectation and the data. In Fig. 2, a small excess of the data over the expectation is observed in the range of medium lepton p_{T} (upper row), towards larger number of jets (middle left), and at small values of maximum $|\eta_{\mathrm{jet}}|$. In this region the relative contribution from $\mathrm{t\bar{t}Z}$+tWZ is large.

The expectations for signals and most background processes are taken from the MC simulations described in Section 3, while the nonprompt contribution is estimated from the data as described above. To validate the estimation of the nonprompt-lepton contribution, events outside the Z boson resonance region are selected, $|m(\ell^{+}\ell^{-}) - m(\mathrm{Z})| > 20\,\mathrm{GeV}$. In this region, the contribution from events with nonprompt leptons is enhanced. Event distributions in this control region are shown in Fig. 4. The data are well described by the sum of the simulations and the contribution from nonprompt leptons as determined from the data.

To obtain an optimal separation between signals and backgrounds, a DNN based on TENSORFLOW (v2) [52] interfaced with KERAS [53] is used to categorize the events into three output nodes. In total, 26 variables are used as input to the DNN. These include kinematic properties of leptons, jets, and the reconstructed top quark candidates, as well as jet and b jet multiplicities, and $\vec{p}_{\mathrm{T}}^{\,\mathrm{miss}}$.

For top quark candidates with a lepton in the final state, the neutrino kinematics are reconstructed from the measured $\vec{p}_{\mathrm{T}}^{\,\mathrm{miss}}$ and the charged lepton originating from the W boson decay, using the W boson mass as a constraint [54]. Depending on the jet multiplicity of the event, three different cases are considered: in events with two jets, of which at least one is a b jet, the leptonic top quark candidate is reconstructed from the lepton, the neutrino momentum, and a b jet; in events with three or more jets, of which at least one is a b jet, squared distances χ^2 of the reconstructed top quark mass with respect to the expected top quark mass 172.69 GeV [54], weighted by their uncertainties, are calculated for both the ℓ+jets and all-hadronic top quark reconstructions; in events with four or more jets, two top quarks can be fully reconstructed and the overall χ^2 value is determined as the sum of the two χ^2 terms. In all cases, the combination of jets that gives the smallest overall χ^2 is taken as the solution.

For the training of the DNN, MC simulation samples of signals and backgrounds are used. The samples are divided into two equal parts, based on even and odd event numbers. For each of these two halves, 80% is used for training, the remaining 20% is used for testing and the other half is used to evaluate the model in order to build the output score distributions that will be used in the final stage of the analysis. The model trained on odd-numbered events is used to evaluate the even-numbered subsample, and vice versa, ensuring an unbiased evaluation. In the case of data, the events are simply divided into two halves, with each half assigned to one of the two models. The three output score values are normalized such that for each event their sum gives unity. In Fig. 5, the data are compared to the expectation. Towards large values of the respective scores, high purities in $\mathrm{t\bar{t}Z}$+tWZ, tZq, and background are achieved.

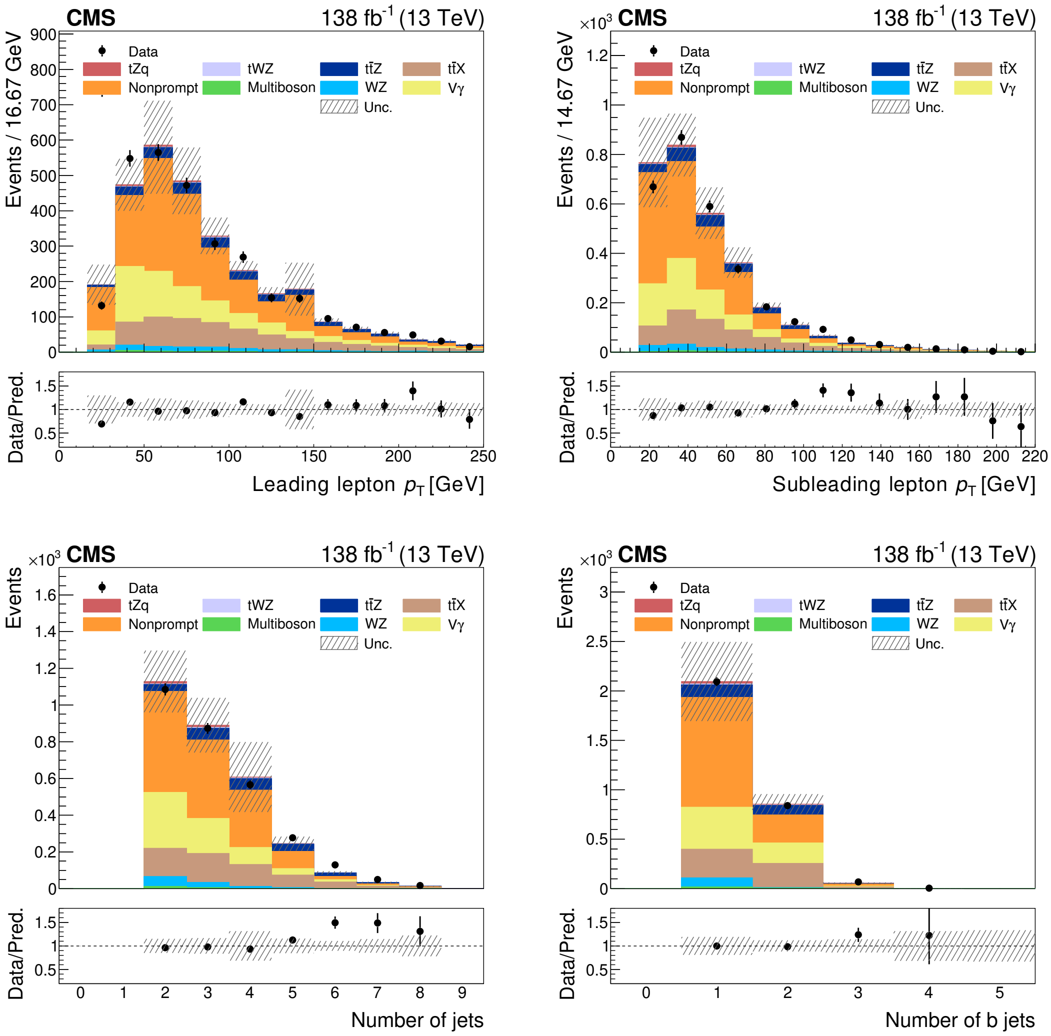

Figure 4: Distributions for events selected in the region with $|m(\ell^+\ell^-) - m(\mathrm{Z})| > 20\,\mathrm{GeV}$ for: the p_T of the lepton with the highest (upper left) and second highest (upper right) p_T, the number of jets (lower left), and the number of b jets (lower right). The data are displayed as points with statistical error bars and the expectation is shown with a histogram with the systematic uncertainty given by the hatched area.

5 Systematic uncertainties

Systematic uncertainties arise from experimental uncertainties in the detector response, such as calibrations, resolutions, and efficiencies, in the integrated luminosity, and from modeling uncertainties, which can affect the efficiency and acceptance. Depending on the type of uncertainty, different shapes are assumed for the prior probability density functions. A given systematic uncertainty can affect both the shape and the normalization of the distribution, or only the normalization. To determine the effect of the uncertainty on the distribution, the analysis is repeated for each source of uncertainty, shifting the relevant uncertainty parameter by one standard deviation. The systematic uncertainties are described in the following and their quantitative impacts on the inclusive $\mathrm{t\bar{t}Z}$+tWZ and tZq cross sections are listed in Table 1. These are obtained by freezing the corresponding group of nuisance parameters in the fit and then subtracting in quadrature the resulting uncertainty from the uncertainty returned by the nominal fit.

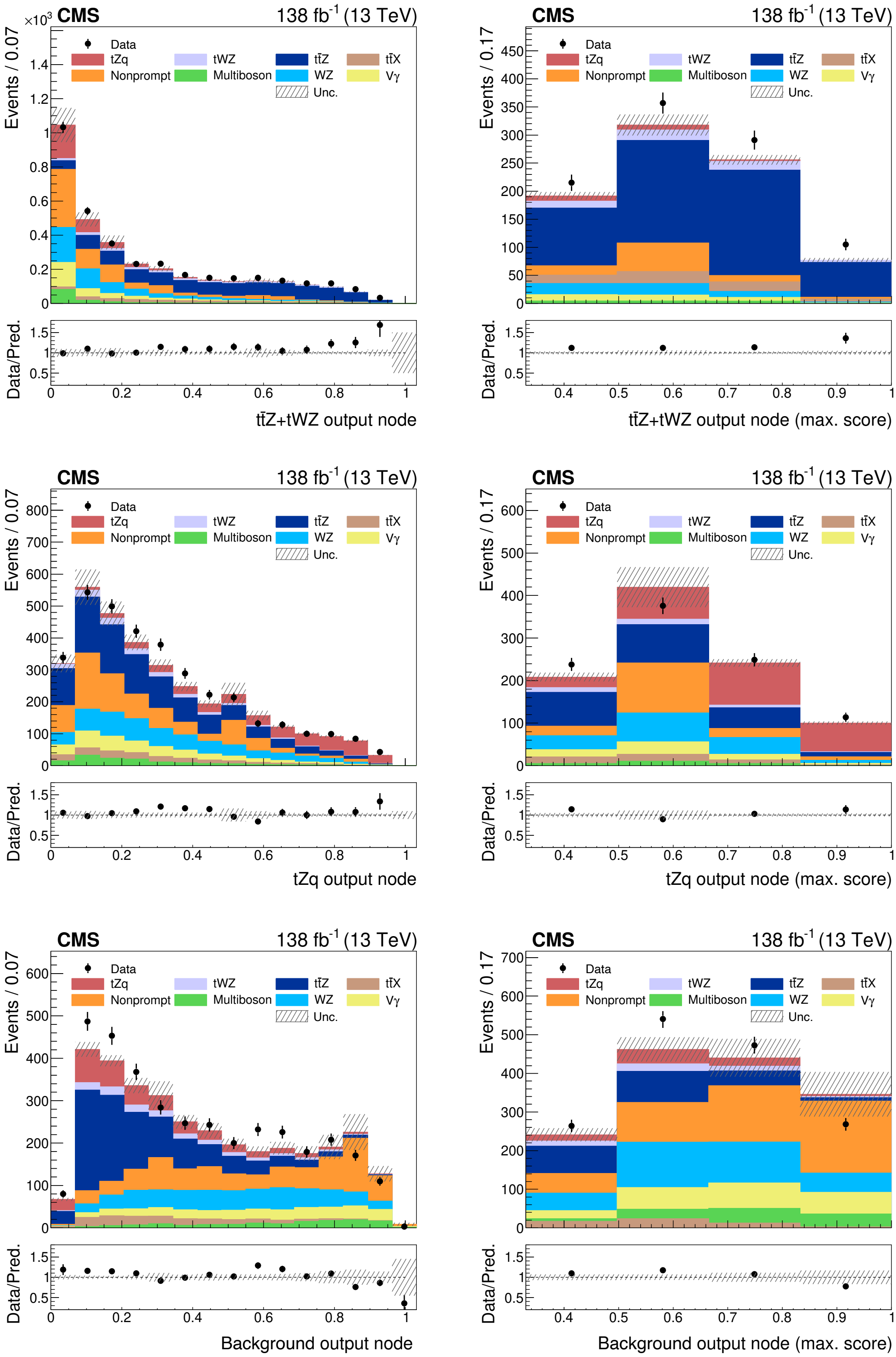

Figure 5: Distributions of the output values in the three DNN output nodes for the sum of $t\bar{t}Z$ and tWZ (upper), tZq (middle), and background (lower). The data are compared with expectations. In the left column, the inclusive distributions are shown, i.e., each selected event enters each of the output nodes. In the right column, each event enters exactly one of the three distributions, namely the one for which the output score is largest. The data are displayed as points with statistical error bars and the expectation is shown with a histogram with the systematic uncertainty given by the hatched area.

Table 1: Systematic uncertainty sources and their relative impact on the inclusive $t\bar{t}Z$+tWZ and tZq cross section measurements.

Source	$\sigma(t\bar{t}Z+tWZ)$	$\sigma(tZq)$
Trigger	2%	2%
Trigger prefiring	<1%	2%
Lepton identification efficiencies	1%	2%
Jet energy scale	1%	3%
Jet energy resolution	<1%	1%
b tagging	1%	2%
Missing transverse momentum	<1%	3%
Nonprompt background	2%	3%
Pileup	<1%	1%
Integrated luminosity	2%	2%
Statistical	3.7%	10%
WZ background modeling	2%	4%
Factorization scale	1%	1%
Renormalization scale	1%	2%
Parton shower	<1%	2%
PDF and strong coupling α_S	<1%	<1%
Underlying event and color reconnection	1%	2%
tWZ modeling	<1%	<1%
MC statistical	<1%	1%
Total	6%	13%

5.1 Experimental uncertainties

The trigger efficiency is found to be close to unity. No trigger SFs are applied, and a flat 2% uncertainty, uncorrelated across the years, is applied per event to account for the uncertainty in the trigger efficiency. During certain periods of the data taking, the so-called *Level-1 trigger prefiring*, i.e., a time jitter of the trigger signal in the muon [55] and ECAL [56] systems, led to a loss of events at the level of 0.5% or less.

The lepton identification efficiencies are treated separately for electrons and muons. As described in Section 4, the simulation is corrected to the data using SFs. The systematic components of the uncertainties are treated as correlated across the data-taking years.

The jet energy scale and resolution uncertainties (JES and JER) include various components [36]. For each of these components, the four-momenta of the jets, as well as the SF for the b tagging efficiencies, are varied and the analysis is repeated.

b tagging: separate SFs and uncertainties are applied for jets originating from bottom and charm quarks, and those from light quarks or gluons [37].

Missing transverse momentum: the observable $\vec{p}_T^{miss}$ includes contributions from jets and unclustered energy in the calorimeters, with systematic uncertainties determined for both components. Jets are considered only if their uncorrected p_T is larger than 15 GeV and their electromagnetic energy fraction is less than 0.9. The uncertainty in the unclustered

$p_{\mathrm{T}}^{\mathrm{miss}}$ is taken as uncorrelated between the years. The uncertainty due to the jets includes each of the JES and JER variations [38].

Nonprompt-lepton background estimation: the uncertainties in the lepton misidentification rates and the statistical uncertainties on the transfer factors are propagated into the final histogram templates, and these are included as shape uncertainties in the fit. Additionally, a 30% uncorrelated bin-by-bin normalization uncertainty is added to account for any residual mismodeling.

Pileup: before applying the event selection, event weights are applied to the MC simulation to match the pileup distributions of the data. Subsequently, to estimate the pileup uncertainty, the pp inelastic cross section [57] is varied by $\pm 4.6\%$, which corresponds to a variation of one standard deviation. This uncertainty is considered as fully correlated across the years.

The integrated luminosities for the 2016, 2017, and 2018 data-taking periods have individual uncertainties of 1.2–2.5% [58–60]. The combined uncertainty for the full data taking period is 1.6%.

5.2 Modeling uncertainties

Backgrounds other than the nonprompt background are modeled using MC simulation samples and an uncertainty of 15% is estimated, except for the $V\gamma$ process, for which a normalization uncertainty of 40% is taken.

Factorization and renormalization scale uncertainties are considered for the signal samples $t\bar{t}Z$, tWZ, and tZq, as well as the background sample WZ. For each process the renormalization and factorization scales are varied independently and the resulting variations are treated as uncorrelated between the different processes.

Parton shower uncertainties are computed by varying the renormalization scale for initial- and final-state radiation (ISR and FSR, respectively) independently. These uncertainties are considered for the processes tZq, $t\bar{t}Z$, tWZ, and WZ. The ISR uncertainty is treated as uncorrelated between the processes, while only two nuisances are considered for FSR, one for the signal samples and one for the WZ process.

PDF and strong coupling α_S uncertainties are considered for the signal samples and for the main background WZ. For each event, 100 eigenvectors and two α_S variations are provided [61], all of them treated as different nuisances in the fit. These uncertainties are considered correlated across the years and between the processes.

Underlying event tune and color reconnection uncertainties are estimated using dedicated MC samples [42, 62]. The uncertainties are treated as correlated among years and processes.

tWZ modeling: two different schemes (DR1 and DR2) are used in the MC generation of tWZ in order to account for the uncertainty due to interference between the $t\bar{t}Z$ and the tWZ processes. The interference between tZq and tWZ is small and not considered in this analysis.

The statistical uncertainty of the MC simulation samples is considered using the Barlow–Beeston lite approach [63].

The relative contribution of the $t\bar{t}Z$ and tWZ processes in their sum was also investigated as a possible source of systematic uncertainty by varying the theoretical assumptions on the cross sections by their maximum uncertainty, approximately 10 fb. This variation is performed anti-correlated between $t\bar{t}Z$ and tWZ, representing the most conservative estimate. However, the resulting effect, estimated to be 0.3% for the inclusive measurement and ranging from 0.1 to 0.5% for differential distributions, is found to be negligible at the current level of precision, and is not included in the fit.

6 Results

The cross sections are measured using a profile likelihood ratio, in which for each cross section hypothesis the optimal nuisance parameters are determined from a fit using the CMS statistical analysis tool COMBINE [64]. For the simultaneous measurement of the sum of the inclusive $t\bar{t}Z$ and tWZ cross sections, and the inclusive tZq cross section, two parameters of interest are used and their best fit values are the result of the measurement. Correspondingly, for the simultaneous measurement of the differential cross sections, the number of parameters of interest in the fit is twice the number of bins of the differential measurement.

6.1 Inclusive cross sections

For the inclusive cross sections, the three-lepton event selection described above is extended to include a category of events with four leptons, as well as a category of three-lepton events without b jets. The region with four leptons and at least one b jet has a high purity in $t\bar{t}Z$ events, as can be seen in Fig. 6 (left), where the b jet multiplicity distribution for this region is shown. The region without b jets is enriched in WZ background events and is useful as a control region. The jet multiplicity distribution for this region is shown in Fig. 6 (right).

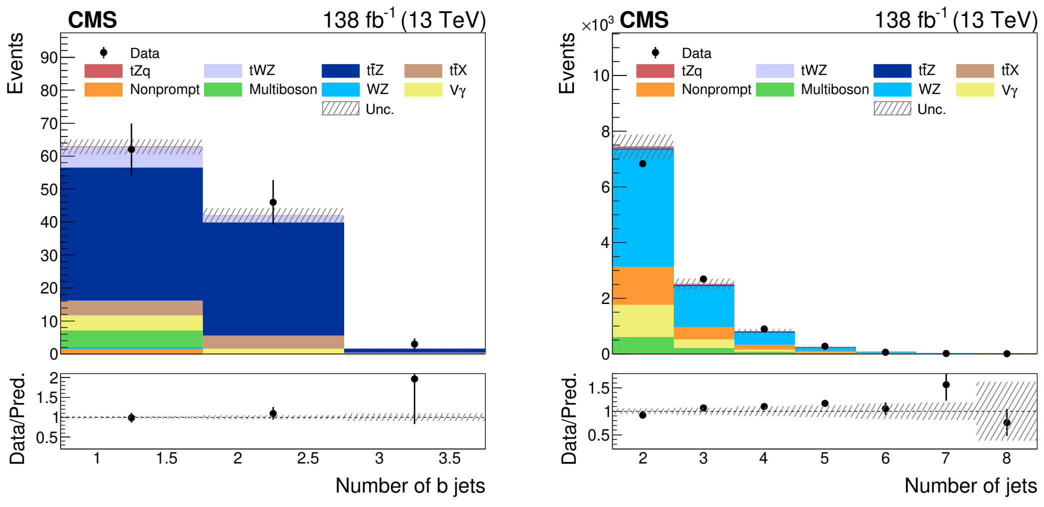

Figure 6: Distributions of the b jet multiplicity in the four lepton region (left) and the jet multiplicity in the zero b jet control region (right). The data are compared to the expectation. The data are displayed as points with statistical error bars and the expectation is shown with a histogram with the systematic uncertainty given by the hatched area.

Both distributions shown in Fig. 6, as well as the three distributions in the right column of Fig. 5, are included in the profile likelihood fit for the extraction of the inclusive cross sections. The b jet multiplicity distribution in the region with four leptons adds sensitivity to the $t\bar{t}Z$

cross section, and the jet multiplicity in the region without b jets improves the modeling of the WZ background.

We define the inclusive cross sections for top quark production in association with a Z boson in the phase space including resonant and nonresonant production of opposite-sign and same-flavor lepton pairs with an invariant mass $70 < m_{\ell^+\ell^-} < 110\,\text{GeV}$. The predicted cross sections in this phase space, as evaluated from the signal generator MADGRAPH5_aMC@NLO, are 0.84 ± 0.08 pb, 0.14 ± 0.01 pb, and 0.82 ± 0.05 pb, for the $\mathrm{t\bar{t}Z}$, tWZ, and tZq processes, respectively.

The fit yields cross section ratios μ to the central value of the SM predictions of $\mu_{\mathrm{t\bar{t}Z+tWZ}} = 1.17 \pm 0.07$ for the sum of the $\mathrm{t\bar{t}Z}$ and tWZ processes and $\mu_{\mathrm{tZq}} = 0.99 \pm 0.13$ for tZq production. The measured inclusive cross sections are:

$$\sigma(\mathrm{t\bar{t}Z{+}tWZ}) = 1.14 \pm 0.05\,(\text{stat}) \pm 0.04\,(\text{syst})\,\text{pb},$$
$$\sigma(\mathrm{tZq}) = 0.81 \pm 0.07\,(\text{stat}) \pm 0.06\,(\text{syst})\,\text{pb}.$$

The distributions resulting from the fit, in the following referred to as postfit distributions, are shown in Fig. 7. The corresponding prefit distributions, i.e., before the scaling of the expectations to the result of the fit, are presented in the right column of Fig. 5 and in Fig. 6.

While the measured tZq cross section agrees very well with the prediction, the sum of the $\mathrm{t\bar{t}Z}$+tWZ cross sections is somewhat higher than the prediction. The two-dimensional profile likelihood ratio for $\mu_{\mathrm{t\bar{t}Z+tWZ}}$ and μ_{tZq} is displayed in Fig. 8. A small positive correlation can be seen, which arises from the correlated sources, such as the experimental uncertainties in JES, lepton identification, luminosity, and trigger.

The previous CMS measurement of the tZq cross section [15] was performed using the same data set as this analysis, but the results were reported in the phase space in which the Z boson decays into two charged leptons (electrons, muons, or tau leptons) with an invariant mass greater than 30 GeV. In this phase space, the current fit yields $93\,^{+12}_{-11}$ fb for the tZq process when fixing the $\mathrm{t\bar{t}Z}$ and tWZ cross sections to their SM predictions, consistent with the previous measurement of $87.9\,^{+10.5}_{-9.5}$ fb [15], and with the prediction 94.2 ± 3.1 fb.

As a cross-check with the previous CMS measurements of the $\mathrm{t\bar{t}Z}$ [14] and tWZ [21] cross sections, we repeat the likelihood fit using two alternative configurations. First, fixing the tZq and tWZ processes to their SM prediction, with normalization uncertainties of 15 and 40%, respectively, returns a value of 0.99 ± 0.07 pb, in agreement with the previous result of 0.95 ± 0.08 pb [14]. Second, constraining the $\mathrm{t\bar{t}Z}$ and tZq processes to the SM prediction with normalization uncertainties of 15% each, the inclusive tWZ cross section is found to be 0.39 ± 0.16 pb, in agreement with the CMS measurement of 0.35 ± 0.11 pb [21].

6.2 Differential measurement

The differential cross sections for the sum of $\mathrm{t\bar{t}Z}$ and tWZ, and for tZq are measured as functions of: the transverse momentum $p_{\mathrm{T}}(\mathrm{Z})$ of the Z boson; the transverse momentum $p_{\mathrm{T}}(\ell_{\mathrm{W}})$ of the lepton coming from the W boson decay; the azimuthal angle $\Delta\phi(\ell^+,\ell^-)$ between the two leptons coming from the Z boson; the ΔR between the Z boson and the lepton coming from the W boson, $\Delta R(\mathrm{Z},\ell_{\mathrm{W}})$; and the cosine of the angle $\cos\theta^*_{\mathrm{Z}}$ between the Z boson and the negatively charged lepton coming from its decay, in the Z boson rest frame. The measured and expected event distributions for these observables have been shown in Fig. 3.

The chosen observables are expected to be sensitive to QCD modeling and/or beyond-SM scenarios and useful for EFT interpretations. For example, $p_{\mathrm{T}}(\mathrm{Z})$ and $p_{\mathrm{T}}(\ell_{\mathrm{W}})$ are sensitive to

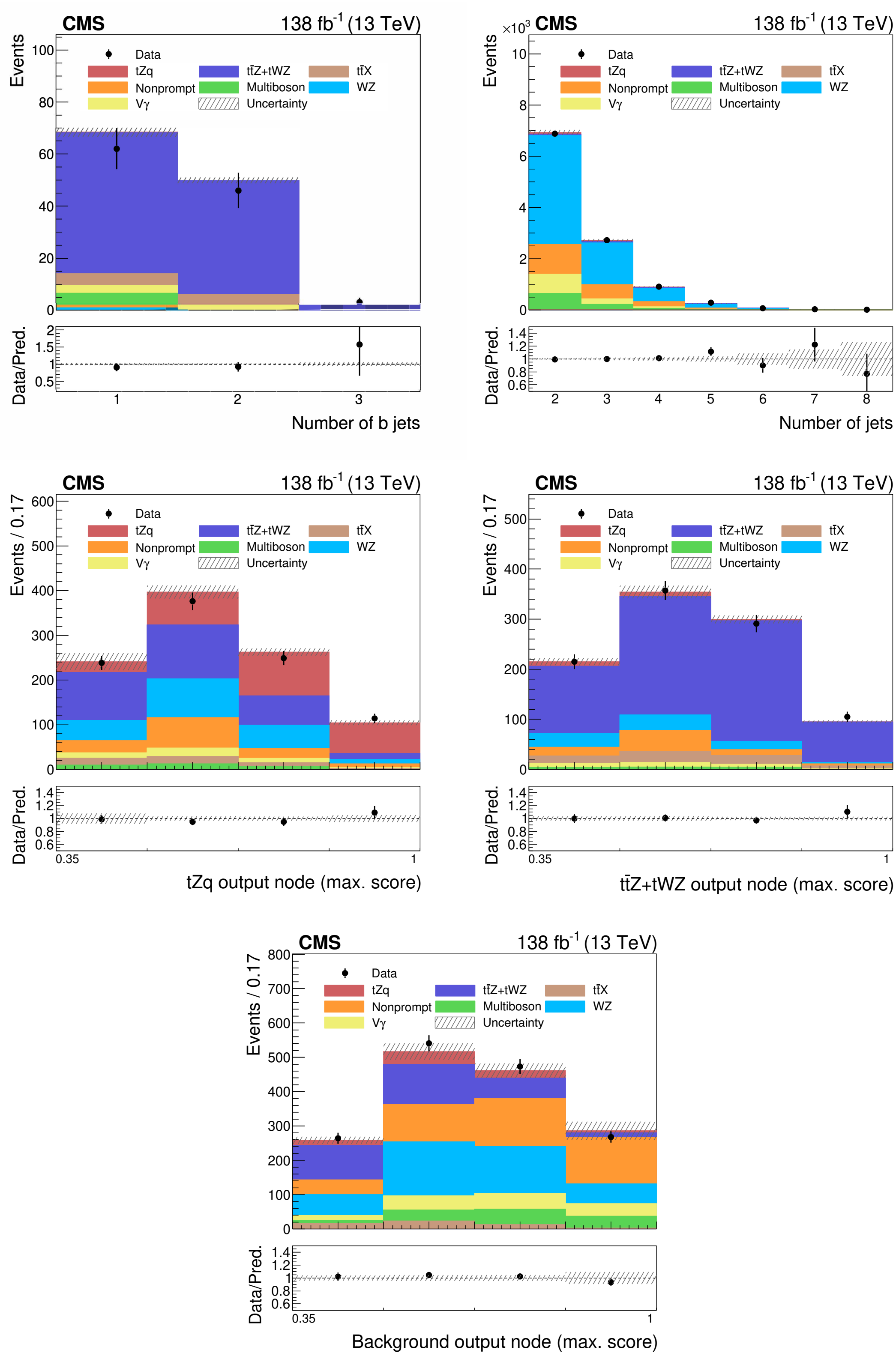

Figure 7: Postfit distributions of the b jet multiplicity in events with four leptons (upper left) and the jet multiplicity distribution in events with zero b jets (upper right). Postfit distributions in the output nodes for tZq (middle left), $t\bar{t}Z$+tWZ (middle right), and the background (lower). The data are displayed as points with statistical error bars and the expectation is shown with a histogram with the systematic uncertainty given by the hatched area.

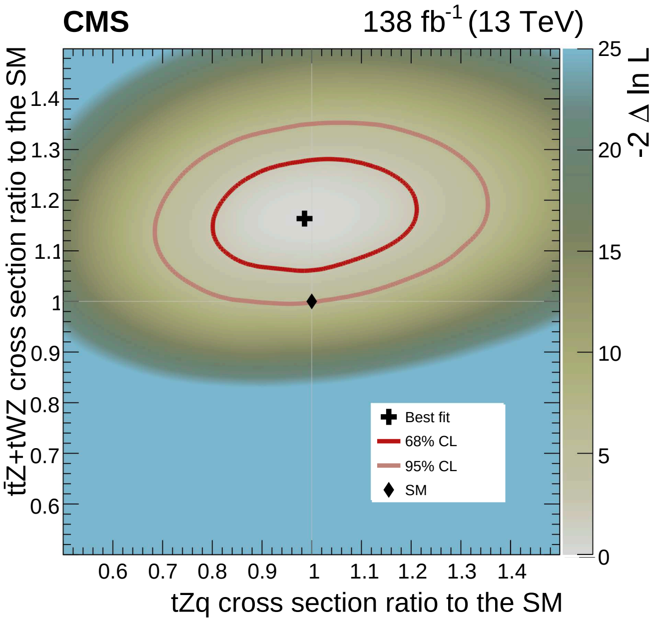

Figure 8: Profile likelihood ratio of the two measured inclusive cross sections normalized to the SM predictions $\mu_{t\bar{t}Z+tWZ}$ and μ_{tZq}. The color axis shows twice the negative log-likelihood difference. The measurement is indicated by a cross, and the SM prediction by a diamond. The 68% and 95% confidence levels (CL) ($-2\Delta\ln L = 2.30$ and 5.99, respectively) are indicated by the red lines.

the $\mathcal{O}_{tW}$ and $\mathcal{O}_{\phi tb}$ operators that describe modified W–t–b couplings [65, 66]. In case of new physics, discrepancies between the data and the SM prediction are expected in $\Delta\phi(\ell^+, \ell^-)$, as the leptons from the Z boson decay will be more or less collimated depending on the boost of the Z boson. The $\Delta R(Z, \ell_W)$ variable is sensitive to the modeling of the processes, as well as to the coupling between top quark and Z boson. The observable $\cos\theta^*_Z$ is an interesting observable to constrain EFT parameters, as discussed in Refs. [14, 67].

The reconstructed observables are affected by the detector resolutions and efficiencies, as well as by limitations in the detector acceptance. The binning of the different observables is chosen by computing a response matrix for both signal samples, maintaining good purity and stability and a sizable number of signal events in each bin. The purity is defined as the fraction of events in a detector-level bin that belong to the corresponding generator-level bin, while the stability is the fraction of events in a generator-level bin that are observed in the corresponding detector-level bin. For all of the observables, the purity and stability are above 85% in every bin. To facilitate comparisons with theory calculations for top quarks in the final state, the data are unfolded to the parton level, after ISR and FSR, and before hadronization.

As described in Section 4, each event is assigned to the process category for which the corresponding output node is maximal. The differential cross sections for tt̄Z and tWZ combined and for tZq are extracted simultaneously using a profile likelihood fit to the data. In each bin of the measurement, templates of the expected output score distributions for signals and backgrounds are created. The signal templates are split into subsamples corresponding to the generator-level bins of the observable to unfold, and the events in the signal output nodes are further split into the different categories corresponding to the detector-level bins. In the fit, for each bin, two cross section parameters of interest are used to determine the likelihood ratio in that bin. The postfit results in each bin are the values of the cross section and nuisance parameters for which the profile likelihood ratio is maximized.

The inputs and results of the fit are shown in Figs. 9 and 10 for the example of the differential cross sections as a function of $p_{\mathrm{T}}(\mathrm{Z})$. The components $\mathrm{t\bar{t}Z}$+tWZ and tZq are measured simultaneously, i.e., eight parameters of interest are determined at the same time.

The differential cross sections for the sum of $\mathrm{t\bar{t}Z}$ and tWZ, and for tZq are shown in Figs. 11 and 12. These figures also include the predictions as obtained from the MC simulation, together with their uncertainties. The uncertainties in the predictions are estimated by summing in quadrature the systematic uncertainties coming from the renormalization and factorization scales, PDFs, and parton showers. For the sum of the $\mathrm{t\bar{t}Z}$ and tWZ cross sections, the uncertainties related to the overlap removal are also included. The predicted cross sections refer to the same phase space as the inclusive measurement. To simplify shape comparisons and to remove bin-to-bin correlated uncertainties, Figs. 13 and 14 show the normalized cross sections. Covariance matrices for the differential cross sections are provided in Fig. 15.

As for the inclusive results, the tZq differential cross sections are in good agreement with the theory prediction. For the sum of the $\mathrm{t\bar{t}Z}$ and tWZ cross sections, an excess over expectation is observed (left columns of Figs. 11 and 12). A possible trend is observed as a function of $p_{\mathrm{T}}(\ell_{\mathrm{W}})$, as presented in Figs. 11 and 13 (middle left), which leads to a discrepancy in the region of low $p_{\mathrm{T}}(\ell_{\mathrm{W}})$. This trend is reminiscent of similar trends in inclusive $\mathrm{t\bar{t}}$ production between MC simulations at NLO and data [14, 21]. For $\mathrm{t\bar{t}}$ production, it has been shown that calculations at next-to-next-to-leading order give a significantly improved description of the data [68–70].

7 Summary

A first simultaneous measurement of single and pair production of top quarks in association with a Z boson is presented. The data were recorded by the CMS experiment in proton-proton collisions at a center-of-mass energy of 13 TeV, corresponding to an integrated luminosity of 138 fb^{-1}. Events with three or more leptons (electrons or muons) are analysed. The separation between the signals is achieved using a deep neural network classifier with three output nodes for the combined $\mathrm{t\bar{t}Z}$ and tWZ processes, the tZq process, and the backgrounds. The inclusive cross sections are measured to be $\sigma(\mathrm{t\bar{t}Z{+}tWZ}) = 1.14 \pm 0.07\,\mathrm{pb}$ for the sum of the tWZ and $\mathrm{t\bar{t}Z}$ processes, and $\sigma(\mathrm{tZq}) = 0.81 \pm 0.10\,\mathrm{pb}$ for tZq production. Both results are evaluated for a dilepton invariant mass between 70 and 110 GeV. The cross sections are measured differentially as functions of several observables. Good agreement with theoretical predictions is found for the tZq process, while for $\mathrm{t\bar{t}Z}$+tWZ production, the slope in the transverse momentum distribution of the lepton that originates from the W boson is found to be somewhat steeper than predicted.

Acknowledgments

We congratulate our colleagues in the CERN accelerator departments for the excellent performance of the LHC and thank the technical and administrative staffs at CERN and at other CMS institutes for their contributions to the success of the CMS effort. In addition, we gratefully acknowledge the computing centers and personnel of the Worldwide LHC Computing Grid and other centers for delivering so effectively the computing infrastructure essential to our analyses. Finally, we acknowledge the enduring support for the construction and operation of the LHC, the CMS detector, and the supporting computing infrastructure provided by the following funding agencies: SC (Armenia), BMBWF and FWF (Austria); FNRS and

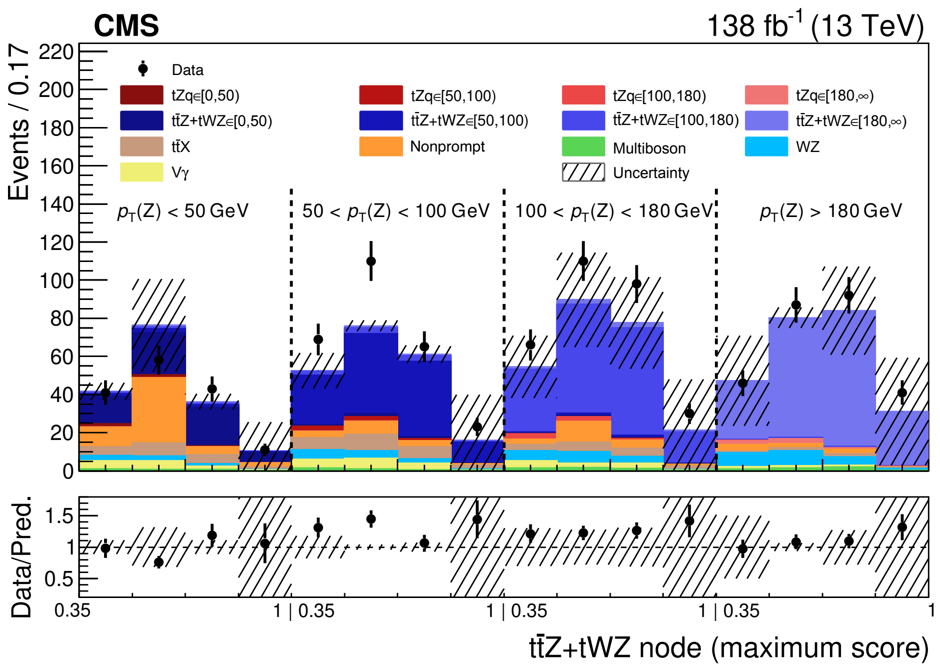

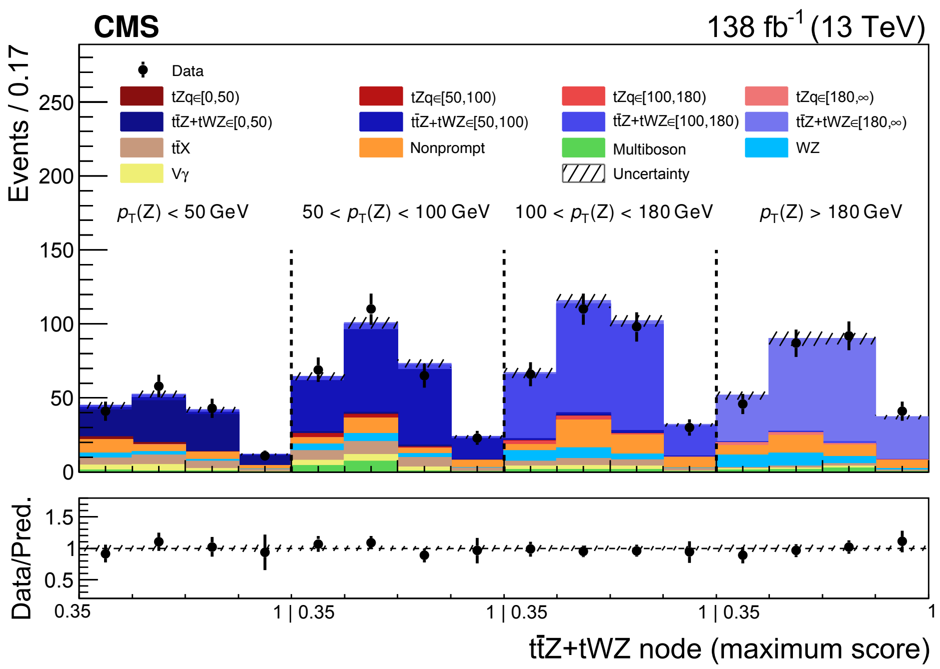

Figure 9: Prefit (upper) and postfit (lower) output node distributions for the sum of the $t\bar{t}Z$ and tWZ processes. Separate templates are shown for each bin of reconstructed $p_T(Z)$. The signal samples are further split into four components each, shown by different colors, according to the generator-level bins of $p_T(Z)$. The fit is performed simultaneously on this distribution and that in Fig. 10. The data are displayed as points with statistical error bars and the expectation is shown with a histogram with the systematic uncertainty given by the hatched area.

FWO (Belgium); CNPq, CAPES, FAPERJ, FAPERGS, and FAPESP (Brazil); MES and BNSF (Bulgaria); CERN; CAS, MoST, and NSFC (China); MINCIENCIAS (Colombia); MSES and CSF (Croatia); RIF (Cyprus); SENESCYT (Ecuador); ERC PRG, RVTT3 and MoER TK202 (Estonia);

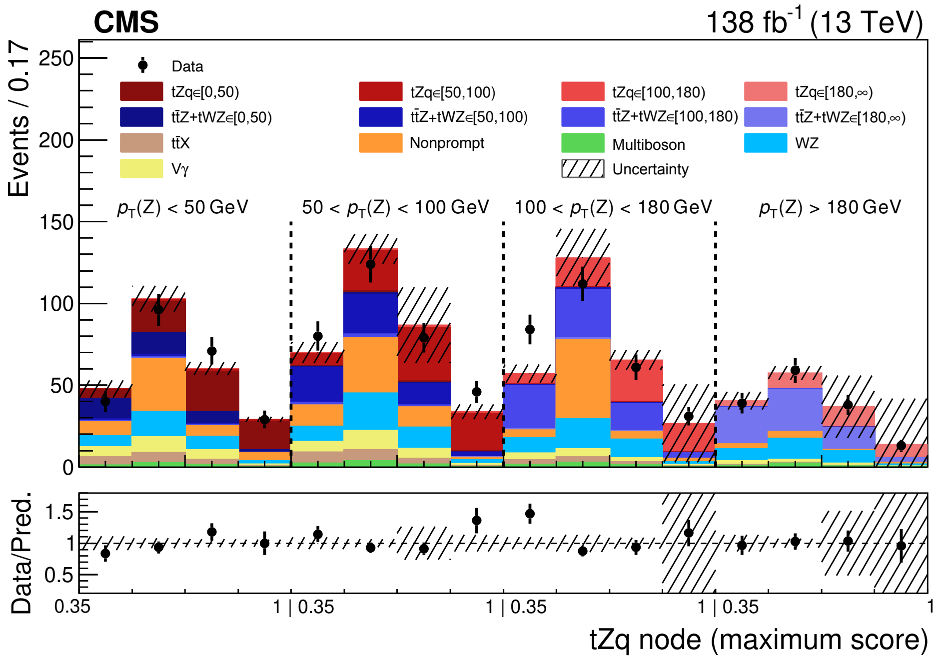

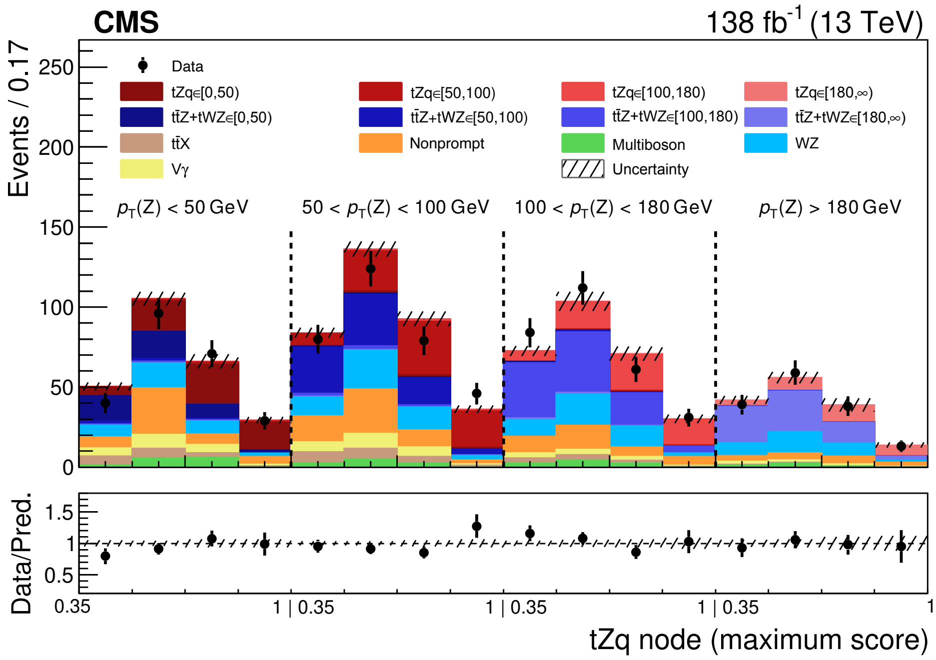

Figure 10: Prefit (upper) and postfit (lower) output node distributions for the tZq process. Separate templates are shown for each bin of reconstructed $p_T(Z)$. The signal samples are further split into four components each, shown by different colors, according to the generator-level bins of $p_T(Z)$. The fit is performed simultaneously on this distribution and that in Fig. 9. The data are displayed as points with statistical error bars and the expectation is shown with a histogram with the systematic uncertainty given by the hatched area.

Academy of Finland, MEC, and HIP (Finland); CEA and CNRS/IN2P3 (France); SRNSF (Georgia); BMBF, DFG, and HGF (Germany); GSRI (Greece); NKFIH (Hungary); DAE and DST (India); IPM (Iran); SFI (Ireland); INFN (Italy); MSIP and NRF (Republic of Korea); MES (Latvia);

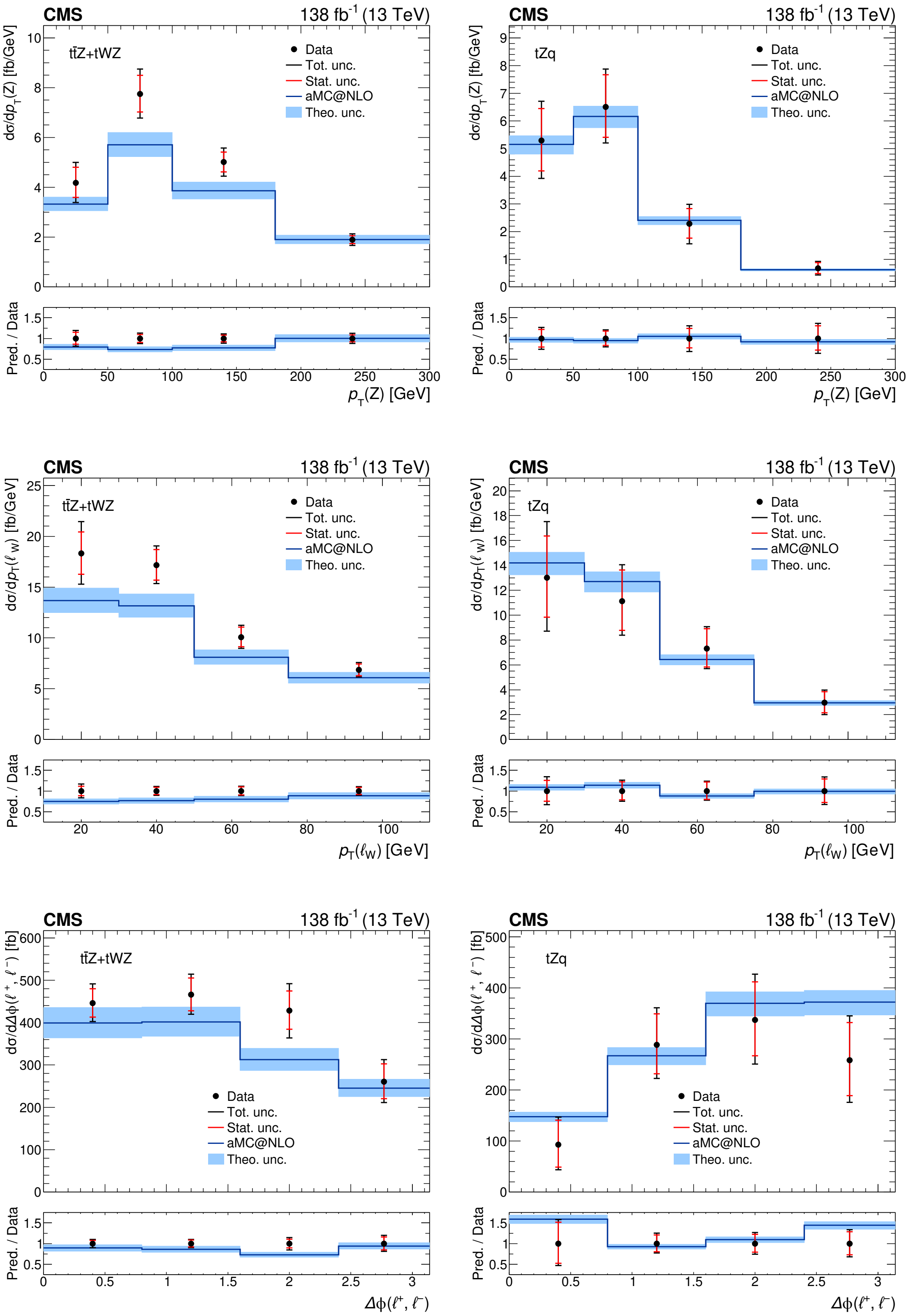

Figure 11: Differential cross sections for the sum of $\mathrm{t\bar{t}Z}$ and tWZ production (left column) and tZq production (right column) as a function of $p_T(Z)$ (upper), $p_T(\ell_W)$ (middle), and $\Delta\phi(\ell^+, \ell^-)$ (lower). The inner (outer) error bars indicate the statistical (total) uncertainty, while the shaded area refers to the uncertainty in the theory prediction. The lower panel shows the ratio of the prediction with the data. The points at unity show the uncertainty of the data.

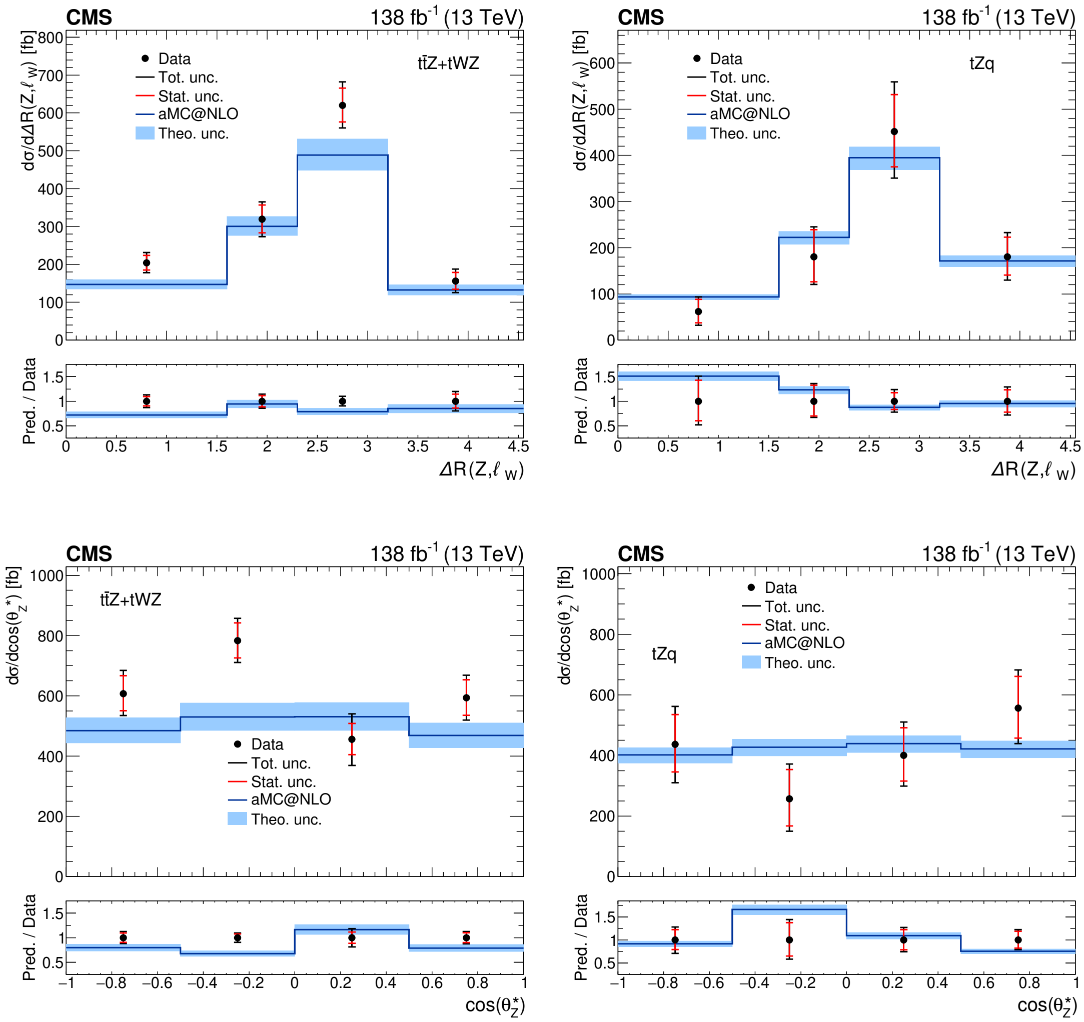

Figure 12: Differential cross sections for the sum of $\mathrm{t\bar{t}Z}$ and tWZ production (left column) and tZq production (right column) as a function of $\Delta R(\mathrm{Z}, \ell_{\mathrm{W}})$ (upper), and $\cos\theta^{*}_{\mathrm{Z}}$ (lower). The inner (outer) error bars indicate the statistical (total) uncertainty, while the shaded area refers to the uncertainty in the theory prediction. The lower panel shows the ratio of the prediction with the data. The points at unity show the uncertainty of the data.

LMTLT (Lithuania); MOE and UM (Malaysia); BUAP, CINVESTAV, CONACYT, LNS, SEP, and UASLP-FAI (Mexico); MOS (Montenegro); MBIE (New Zealand); PAEC (Pakistan); MES and NSC (Poland); FCT (Portugal); MESTD (Serbia); MCIN/AEI and PCTI (Spain); MOSTR (Sri Lanka); Swiss Funding Agencies (Switzerland); MST (Taipei); MHESI and NSTDA (Thailand); TUBITAK and TENMAK (Turkey); NASU (Ukraine); STFC (United Kingdom); DOE and NSF (USA).

Individuals have received support from the Marie-Curie program and the European Research Council and Horizon 2020 Grant, contract Nos. 675440, 724704, 752730, 758316, 765710, 824093, 101115353, 101002207, and COST Action CA16108 (European Union); the Leventis Foundation; the Alfred P. Sloan Foundation; the Alexander von Humboldt Foundation; the Science Committee, project no. 22rl-037 (Armenia); the Belgian Federal Science Policy Office; the Fonds pour la Formation à la Recherche dans l'Industrie et dans l'Agriculture (FRIA-Belgium); the F.R.S.-FNRS and FWO (Belgium) under the "Excellence of Science – EOS" – be.h project n.

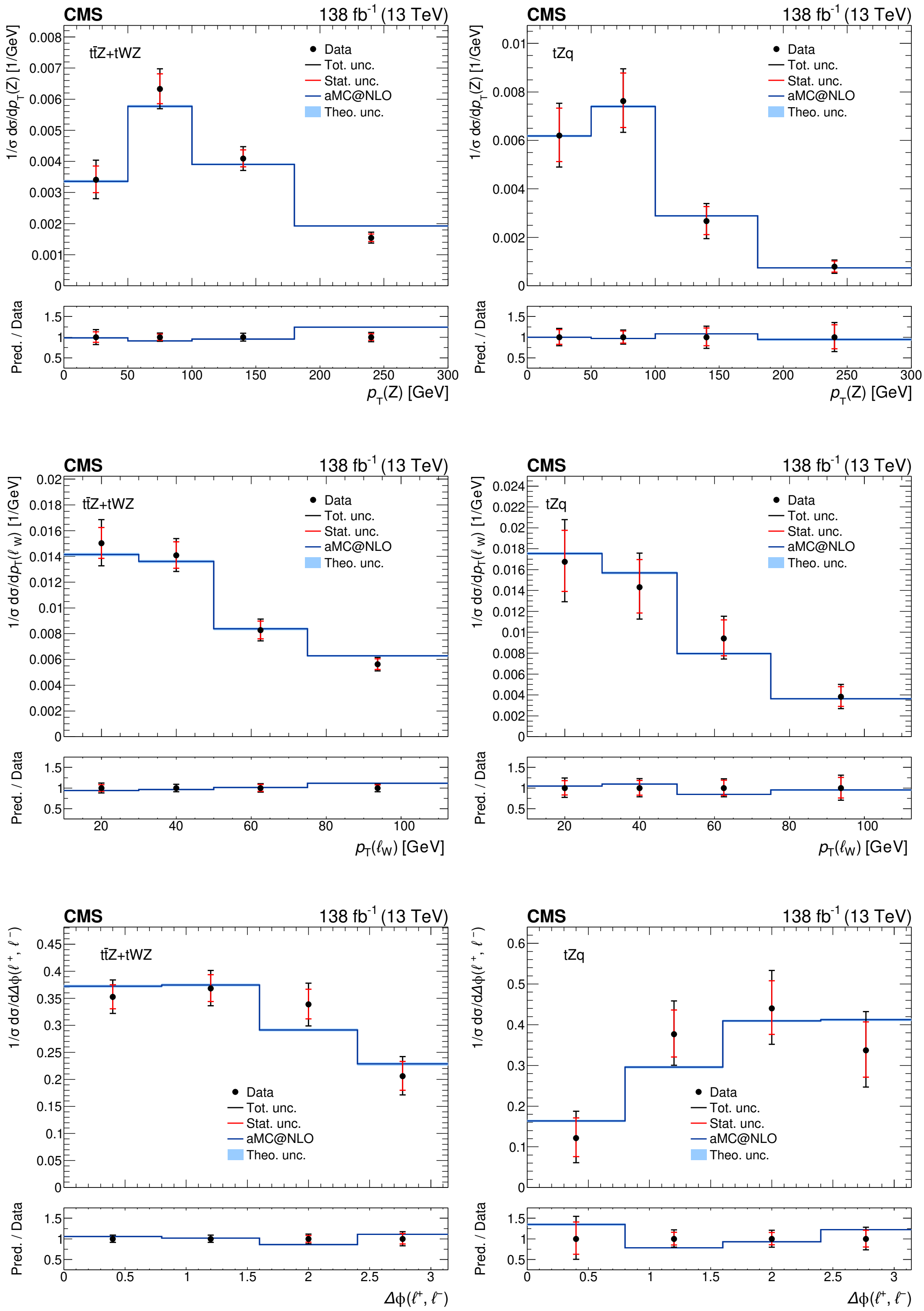

Figure 13: Normalized differential cross sections for the sum of $t\bar{t}Z$ and tWZ production (left column) and tZq production (right column) as a function of $p_T(Z)$ (upper), $p_T(\ell_W)$ (middle), and $\Delta\phi(\ell^+, \ell^-)$ (lower). The inner (outer) error bars indicate the statistical (total) uncertainty, while the shaded area refers to the uncertainty in the theory prediction. The lower panel shows the ratio of the prediction with the data. The points at unity show the uncertainty of the data.

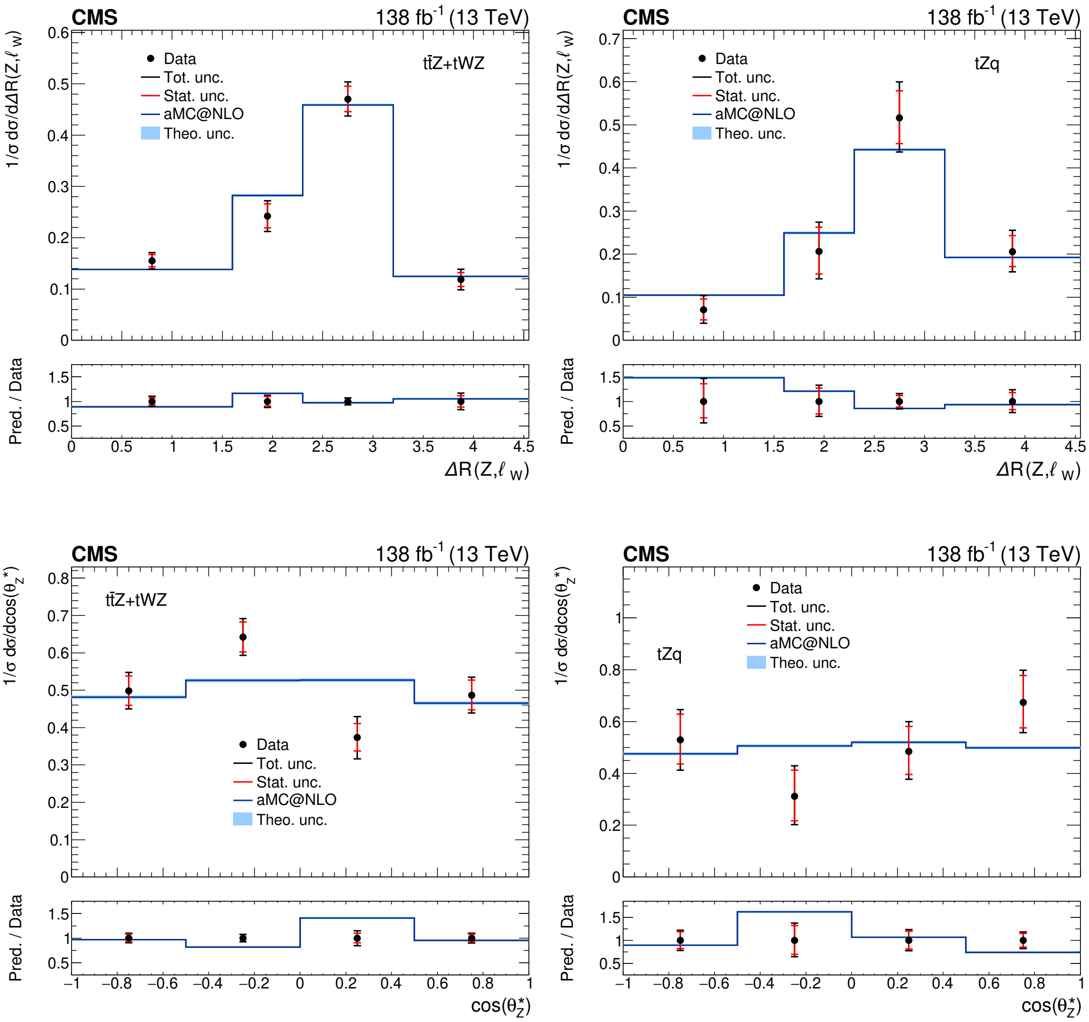

Figure 14: Normalized differential cross sections for the sum of $\mathrm{t\bar{t}Z}$ and tWZ production (left column) and tZq production (right column) as a function of $\Delta R(\mathrm{Z}, \ell_\mathrm{W})$ (upper), and $\cos\theta^*_\mathrm{Z}$ (lower). The inner (outer) error bars indicate the statistical (total) uncertainty, while the shaded area refers to the uncertainty in the theory prediction. The lower panel shows the ratio of the prediction with the data. The points at unity show the uncertainty of the data.

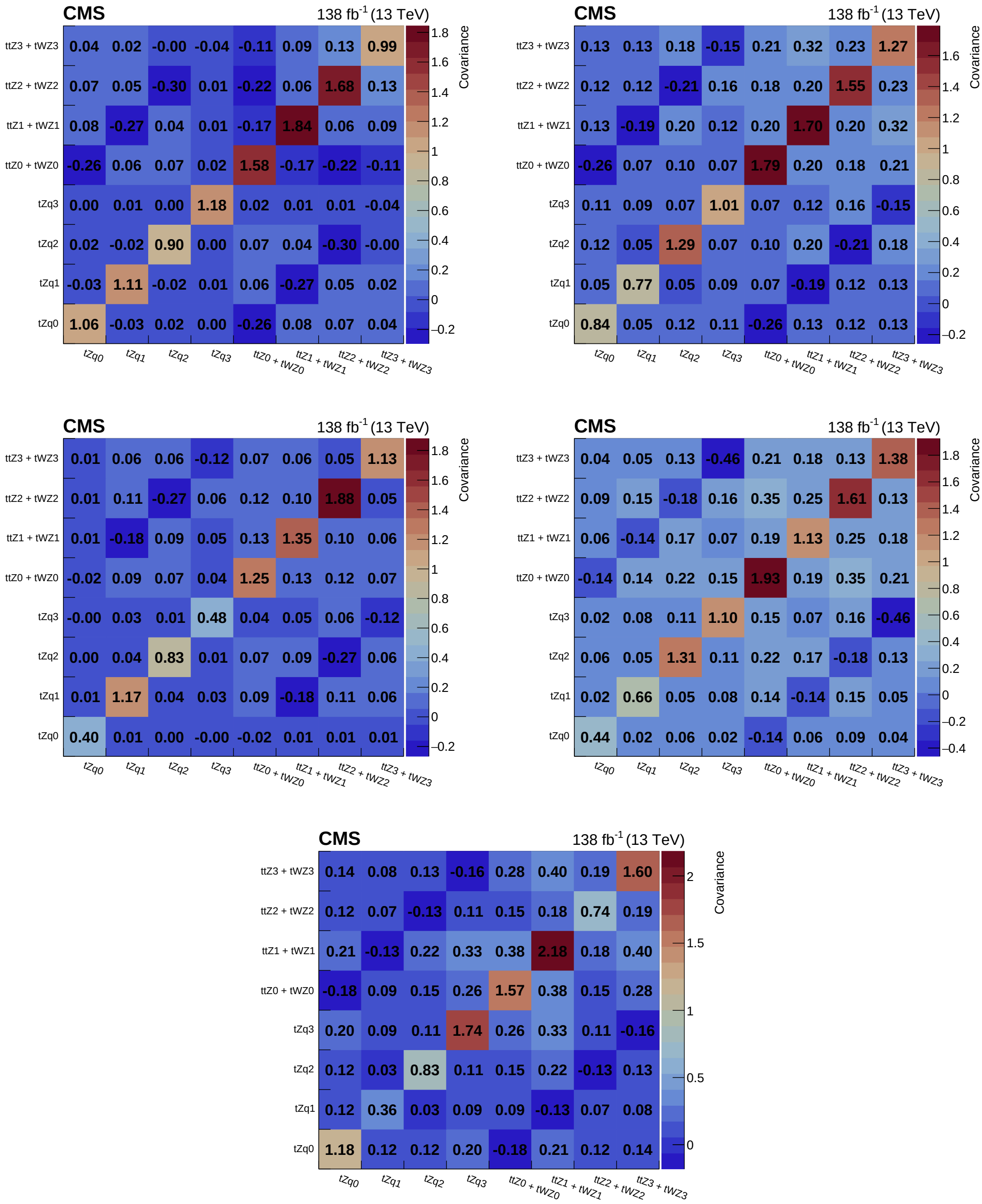

Figure 15: Covariance matrices for the simultaneous measurement of the differential cross section as a function of $p_{\mathrm{T}}(\mathrm{Z})$, (upper left), $p_{\mathrm{T}}(\ell_{\mathrm{W}})$ (upper right), $\Delta R(\mathrm{Z}, \ell_{\mathrm{W}})$ (middle left), $\Delta\phi(\ell^+, \ell^-)$ (middle right), and $\cos\theta^*_{\mathrm{Z}}$ (lower). The last digits in the axis labels refer to the respective bin of the corresponding differential cross section measurement.

30820817; the Beijing Municipal Science & Technology Commission, No. Z191100007219010 and Fundamental Research Funds for the Central Universities (China); the Ministry of Education, Youth and Sports (MEYS) of the Czech Republic; the Shota Rustaveli National Science Foundation, grant FR-22-985 (Georgia); the Deutsche Forschungsgemeinschaft (DFG), among others, under Germany's Excellence Strategy – EXC 2121 "Quantum Universe" – 390833306, and under project number 400140256 - GRK2497; the Hellenic Foundation for Research and Innovation (HFRI), Project Number 2288 (Greece); the Hungarian Academy of Sciences, the New National Excellence Program - ÚNKP, the NKFIH research grants K 131991, K 133046, K 138136, K 143460, K 143477, K 146913, K 146914, K 147048, 2020-2.2.1-ED-2021-00181, and TKP2021-NKTA-64 (Hungary); the Council of Science and Industrial Research, India; ICSC – National Research Center for High Performance Computing, Big Data and Quantum Computing and FAIR – Future Artificial Intelligence Research, funded by the NextGenerationEU program (Italy); the Latvian Council of Science; the Ministry of Education and Science, project no. 2022/WK/14, and the National Science Center, contracts Opus 2021/41/B/ST2/01369 and 2021/43/B/ST2/01552 (Poland); the Fundação para a Ciência e a Tecnologia, grant CEECIND/01334/2018 (Portugal); the National Priorities Research Program by Qatar National Research Fund; MCIN/AEI/10.13039/501100011033, ERDF "a way of making Europe", and the Programa Estatal de Fomento de la Investigación Científica y Técnica de Excelencia María de Maeztu, grant MDM-2017-0765 and Programa Severo Ochoa del Principado de Asturias (Spain); the Chulalongkorn Academic into Its 2nd Century Project Advancement Project, and the National Science, Research and Innovation Fund via the Program Management Unit for Human Resources & Institutional Development, Research and Innovation, grant B39G670016 (Thailand); the Kavli Foundation; the Nvidia Corporation; the SuperMicro Corporation; the Welch Foundation, contract C-1845; and the Weston Havens Foundation (USA).

References

[1] R. Röntsch and M. Schulze, "Constraining couplings of top quarks to the Z boson in $\mathrm{t\bar{t}}$+Z production at the LHC", *JHEP* **07** (2014) 091, doi:10.1007/JHEP07(2014)091, arXiv:1404.1005. [Erratum: doi:10.1007/JHEP09(2015)132].

[2] LHC Higgs Cross Section Working Group, D. de Florian et al., "Handbook of LHC Higgs cross sections: 4. Deciphering the nature of the Higgs sector", CERN Report CERN-2017-002-M, 2016. doi:10.23731/CYRM-2017-002, arXiv:1610.07922.

[3] ATLAS Collaboration, "Measurement of the $\mathrm{t\bar{t}W}$ and $\mathrm{t\bar{t}Z}$ production cross sections in pp collisions at $\sqrt{s} = 8$ TeV with the ATLAS detector", *JHEP* **11** (2015) 172, doi:10.1007/JHEP11(2015)172, arXiv:1509.05276.

[4] ATLAS Collaboration, "Measurement of the $\mathrm{t\bar{t}Z}$ and $\mathrm{t\bar{t}W}$ production cross sections in multilepton final states using 3.2 fb^{-1} of pp collisions at $\sqrt{s} = 13$ TeV with the ATLAS detector", *Eur. Phys. J. C* **77** (2017) 40, doi:10.1140/epjc/s10052-016-4574-y, arXiv:1609.01599.

[5] ATLAS Collaboration, "Measurement of the production cross-section of a single top quark in association with a Z boson in proton-proton collisions at 13 TeV with the ATLAS detector", *Phys. Lett. B* **780** (2018) 557, doi:10.1016/j.physletb.2018.03.023, arXiv:1710.03659.

[6] ATLAS Collaboration, "Measurement of the $t\bar{t}Z$ and $t\bar{t}W$ cross sections in proton-proton collisions at $\sqrt{s} = 13$ TeV with the ATLAS detector", *Phys. Rev. D* **99** (2019) 072009, doi:10.1103/PhysRevD.99.072009, arXiv:1901.03584.

[7] ATLAS Collaboration, "Observation of the associated production of a top quark and a Z boson in pp collisions at $\sqrt{s} = 13$ TeV with the ATLAS detector", *JHEP* **07** (2020) 124, doi:10.1007/JHEP07(2020)124, arXiv:2002.07546.

[8] ATLAS Collaboration, "Measurements of the inclusive and differential production cross sections of a top-quark-antiquark pair in association with a Z boson at $\sqrt{s} = 13$ TeV with the ATLAS detector", *Eur. Phys. J. C* **81** (2021) 737, doi:10.1140/epjc/s10052-021-09439-4, arXiv:2103.12603.

[9] ATLAS Collaboration, "Inclusive and differential cross-section measurements of $t\bar{t}Z$ production in pp collisions at $\sqrt{s} = 13$ TeV with the ATLAS detector, including EFT and spin-correlation interpretations", *JHEP* **07** (2024) 163, doi:10.1007/JHEP07(2024)163, arXiv:2312.04450.

[10] CMS Collaboration, "Observation of top quark pairs produced in association with a vector boson in pp collisions at $\sqrt{s} = 8$ TeV", *JHEP* **01** (2016) 096, doi:10.1007/JHEP01(2016)096, arXiv:1510.01131.

[11] CMS Collaboration, "Measurement of the cross section for top quark pair production in association with a W or Z boson in proton-proton collisions at $\sqrt{s} = 13$ TeV", *JHEP* **08** (2018) 011, doi:10.1007/JHEP08(2018)011, arXiv:1711.02547.

[12] CMS Collaboration, "Measurement of the associated production of a single top quark and a Z boson in pp collisions at $\sqrt{s} = 13$ TeV", *Phys. Lett. B* **779** (2018) 358, doi:10.1016/j.physletb.2018.02.025, arXiv:1712.02825.

[13] CMS Collaboration, "Observation of single top quark production in association with a Z boson in proton-proton collisions at $\sqrt{s} = 13$ TeV", *Phys. Rev. Lett.* **122** (2019) 132003, doi:10.1103/PhysRevLett.122.132003, arXiv:1812.05900.

[14] CMS Collaboration, "Measurement of top quark pair production in association with a Z boson in proton-proton collisions at $\sqrt{s} = 13$ TeV", *JHEP* **03** (2020) 056, doi:10.1007/JHEP03(2020)056, arXiv:1907.11270.

[15] CMS Collaboration, "Inclusive and differential cross section measurements of single top quark production in association with a Z boson in proton-proton collisions at $\sqrt{s} = 13$ TeV", *JHEP* **02** (2022) 107, doi:10.1007/JHEP02(2022)107, arXiv:2111.02860.

[16] J. Campbell, R. K. Ellis, and R. Röntsch, "Single top production in association with a Z boson at the LHC", *Phys. Rev. D* **87** (2013) 114006, doi:10.1103/PhysRevD.87.114006, arXiv:1302.3856.

[17] S. Frixione et al., "Electroweak and QCD corrections to top-pair hadroproduction in association with heavy bosons", *JHEP* **06** (2015) 184, doi:10.1007/JHEP06(2015)184, arXiv:1504.03446.

[18] R. Frederix et al., "The automation of next-to-leading order electroweak calculations", *JHEP* **07** (2018) 185, doi:10.1007/JHEP07(2018)185, arXiv:1804.10017. [Erratum: doi:10.1007/JHEP11(2021)085].

[19] A. Kulesza et al., "Associated top-pair production with a heavy boson production through NLO+NNLL accuracy at the LHC", in *Proc. 54th Rencontres de Moriond on QCD and High Energy Interactions (Moriond QCD 2019): La Thuile, Italy, March 23–30, 2019*, p. 39. 2019. arXiv:1905.07815.

[20] D. Pagani, I. Tsinikos, and E. Vryonidou, "NLO QCD+EW predictions for tHj and tZj production at the LHC", *JHEP* **08** (2020) 082, doi:10.1007/JHEP08(2020)082, arXiv:2006.10086.

[21] CMS Collaboration, "Evidence for tWZ production in proton-proton collisions at $\sqrt{s} = 13$ TeV in multilepton final states", *Phys. Lett. B* **855** (2024) 138815, doi:10.1016/j.physletb.2024.138815, arXiv:2312.11668.

[22] J. Alwall et al., "The automated computation of tree-level and next-to-leading order differential cross sections, and their matching to parton shower simulations", *JHEP* **07** (2014) 079, doi:10.1007/JHEP07(2014)079, arXiv:1405.0301.

[23] H. El Faham, F. Maltoni, K. Mimasu, and M. Zaro, "Single top production in association with a WZ pair at the LHC in the SMEFT", *JHEP* **01** (2022) 100, doi:10.1007/JHEP01(2022)100, arXiv:2111.03080.

[24] W. Buchmuller and D. Wyler, "Effective Lagrangian analysis of new interactions and flavour conservation", *Nucl. Phys. B* **268** (1986) 621, doi:10.1016/0550-3213(86)90262-2.

[25] C. P. Burgess, "An introduction to effective field theory", *Ann. Rev. Nucl. Part. Sci.* **57** (2007) 329, doi:10.1146/annurev.nucl.56.080805.140508, arXiv:hep-th/0701053.

[26] SMEFiT Collaboration, "Combined SMEFT interpretation of Higgs, diboson, and top quark data from the LHC", *JHEP* **11** (2021) 089, doi:10.1007/JHEP11(2021)089, arXiv:2105.00006.

[27] N. Castro et al., "LHC EFT WG report: Experimental measurements and observables", LHC EFT Working Group Public Note CERN-LHCEFTWG-2022-001, 2022. arXiv:2211.08353.

[28] HEPData record for this analysis, 2024. doi:10.17182/hepdata.149880.

[29] CMS Collaboration, "The CMS experiment at the CERN LHC", *JINST* **3** (2008) S08004, doi:10.1088/1748-0221/3/08/S08004.

[30] CMS Collaboration, "Development of the CMS detector for the CERN LHC Run 3", *JINST* **19** (2024) P05064, doi:10.1088/1748-0221/19/05/P05064, arXiv:2309.05466.

[31] CMS Collaboration, "Particle-flow reconstruction and global event description with the CMS detector", *JINST* **12** (2017) P10003, doi:10.1088/1748-0221/12/10/P10003, arXiv:1706.04965.

[32] CMS Collaboration, "Technical proposal for the Phase-II upgrade of the Compact Muon Solenoid", CMS Technical Proposal CERN-LHCC-2015-010, CMS-TDR-15-02, 2015. doi:10.17181/CERN.VU8I.D59J.

[33] M. Cacciari, G. P. Salam, and G. Soyez, "The anti-k_T jet clustering algorithm", *JHEP* **04** (2008) 063, doi:10.1088/1126-6708/2008/04/063, arXiv:0802.1189.

[34] M. Cacciari, G. P. Salam, and G. Soyez, "FASTJET user manual", *Eur. Phys. J. C* **72** (2012) 1896, doi:10.1140/epjc/s10052-012-1896-2, arXiv:1111.6097.

[35] CMS Collaboration, "Pileup mitigation at CMS in 13 TeV data", *JINST* **15** (2020) P09018, doi:10.1088/1748-0221/15/09/P09018, arXiv:2003.00503.

[36] CMS Collaboration, "Jet energy scale and resolution in the CMS experiment in pp collisions at 8 TeV", *JINST* **12** (2017) P02014, doi:10.1088/1748-0221/12/02/P02014, arXiv:1607.03663.

[37] CMS Collaboration, "Identification of heavy-flavour jets with the CMS detector in pp collisions at 13 TeV", *JINST* **13** (2018) P05011, doi:10.1088/1748-0221/13/05/P05011, arXiv:1712.07158.

[38] CMS Collaboration, "Performance of missing transverse momentum reconstruction in proton-proton collisions at $\sqrt{s} = 13$ TeV using the CMS detector", *JINST* **14** (2019) P07004, doi:10.1088/1748-0221/14/07/P07004, arXiv:1903.06078.

[39] S. Frixione, P. Nason, and C. Oleari, "Matching NLO QCD computations with parton shower simulations: the POWHEG method", *JHEP* **11** (2007) 070, doi:10.1088/1126-6708/2007/11/070, arXiv:0709.2092.

[40] J. M. Campbell and R. K. Ellis, "MCFM for the Tevatron and the LHC", in *Proc. 10th DESY Workshop on Elementary Particle Theory: Loops and Legs in Quantum Field Theory (LL2010): Wörlitz, Germany, April 25–30, 2010.* 2010. arXiv:1007.3492. [Nucl. Phys. B Proc. Suppl. 205–206 (2010) 10]. doi:10.1016/j.nuclphysbps.2010.08.011.

[41] T. Sjöstrand et al., "An introduction to PYTHIA 8.2", *Comput. Phys. Commun.* **191** (2015) 159, doi:10.1016/j.cpc.2015.01.024, arXiv:1410.3012.

[42] CMS Collaboration, "Extraction and validation of a new set of CMS PYTHIA 8 tunes from underlying-event measurements", *Eur. Phys. J. C* **80** (2020) 4, doi:10.1140/epjc/s10052-019-7499-4, arXiv:1903.12179.

[43] R. Frederix and S. Frixione, "Merging meets matching in MC@NLO", *JHEP* **12** (2012) 061, doi:10.1007/JHEP12(2012)061, arXiv:1209.6215.

[44] J. Alwall et al., "Comparative study of various algorithms for the merging of parton showers and matrix elements in hadronic collisions", *Eur. Phys. J. C* **53** (2008) 473, doi:10.1140/epjc/s10052-007-0490-5, arXiv:0706.2569.

[45] NNPDF Collaboration, "Parton distributions from high-precision collider data", *Eur. Phys. J. C* **77** (2017) 663, doi:10.1140/epjc/s10052-017-5199-5, arXiv:1706.00428.

[46] S. Frixione et al., "Single-top hadroproduction in association with a W boson", *JHEP* **07** (2008) 029, doi:10.1088/1126-6708/2008/07/029, arXiv:0805.3067.

[47] F. Demartin et al., "tWH associated production at the LHC", *Eur. Phys. J. C* **77** (2017) 34, doi:10.1140/epjc/s10052-017-4601-7, arXiv:1607.05862.

[48] GEANT4 Collaboration, "GEANT4—a simulation toolkit", *Nucl. Instrum. Meth. A* **506** (2003) 250, doi:10.1016/S0168-9002(03)01368-8.

[49] CMS Collaboration, "Observation of four top quark production in proton-proton collisions at $\sqrt{s} = 13\,\text{TeV}$", *Phys. Lett. B* **847** (2023) 138290, doi:10.1016/j.physletb.2023.138290, arXiv:2305.13439.

[50] CMS Collaboration, "Electron and photon reconstruction and identification with the CMS experiment at the CERN LHC", *JINST* **16** (2021) P05014, doi:10.1088/1748-0221/16/05/P05014, arXiv:2012.06888.

[51] CMS Collaboration, "Performance of the CMS muon detector and muon reconstruction with proton-proton collisions at $\sqrt{s} = 13\,\text{TeV}$", *JINST* **13** (2018) P06015, doi:10.1088/1748-0221/13/06/P06015, arXiv:1804.04528.

[52] M. Abadi et al., "TENSORFLOW: Large-scale machine learning on heterogeneous systems", 2015. Software available from http://tensorflow.org. doi:10.5281/zenodo.4724125.

[53] F. Chollet et al., "KERAS", 2015. Software available from https://keras.io.

[54] Particle Data Group, R. L. Workman et al., "Review of particle physics", *Prog. Theor. Exp. Phys.* **2022** (2022) 083C01, doi:10.1093/ptep/ptac097.

[55] CMS Collaboration, "Performance of the CMS muon trigger system in proton-proton collisions at $\sqrt{s} = 13\,\text{TeV}$", *JINST* **16** (2021) P07001, doi:10.1088/1748-0221/16/07/P07001, arXiv:2102.04790.

[56] CMS Collaboration, "Performance of the CMS Level-1 trigger in proton-proton collisions at $\sqrt{s} = 13\,\text{TeV}$", *JINST* **15** (2020) P10017, doi:10.1088/1748-0221/15/10/P10017, arXiv:2006.10165.

[57] CMS Collaboration, "Measurement of the inelastic proton-proton cross section at $\sqrt{s} = 13\,\text{TeV}$", *JHEP* **07** (2018) 161, doi:10.1007/JHEP07(2018)161, arXiv:1802.02613.

[58] CMS Collaboration, "Precision luminosity measurement in proton-proton collisions at $\sqrt{s} = 13\,\text{TeV}$ in 2015 and 2016 at CMS", *Eur. Phys. J. C* **81** (2021) 800, doi:10.1140/epjc/s10052-021-09538-2, arXiv:2104.01927.

[59] CMS Collaboration, "CMS luminosity measurement for the 2017 data-taking period at $\sqrt{s} = 13\,\text{TeV}$", CMS Physics Analysis Summary CMS-PAS-LUM-17-004, 2018.

[60] CMS Collaboration, "CMS luminosity measurement for the 2018 data-taking period at $\sqrt{s} = 13\,\text{TeV}$", CMS Physics Analysis Summary CMS-PAS-LUM-18-002, 2019.

[61] J. Butterworth et al., "PDF4LHC recommendations for LHC Run 2", *J. Phys. G* **43** (2016) 023001, doi:10.1088/0954-3899/43/2/023001, arXiv:1510.03865.

[62] S. Argyropoulos and T. Sjöstrand, "Effects of color reconnection on $\mathrm{t\bar{t}}$ final states at the LHC", *JHEP* **11** (2014) 043, doi:10.1007/JHEP11(2014)043, arXiv:1407.6653.

[63] R. Barlow and C. Beeston, "Fitting using finite Monte Carlo samples", *Comput. Phys. Commun.* **77** (1993) 219, doi:10.1016/0010-4655(93)90005-W.

[64] CMS Collaboration, "The CMS statistical analysis and combination tool: COMBINE", 2024. arXiv:2404.06614. Accepted by *Comput. Softw. Big Sci.*

[65] CMS Collaboration, "Probing effective field theory operators in the associated production of top quarks with a Z boson in multilepton final states at $\sqrt{s} = 13$ TeV", *JHEP* **12** (2021) 083, doi:10.1007/JHEP12(2021)083, arXiv:2107.13896.

[66] C. Degrande et al., "Single-top associated production with a Z or H boson at the LHC: the SMEFT interpretation", *JHEP* **10** (2018) 005, doi:10.1007/JHEP10(2018)005, arXiv:1804.07773.

[67] D. Spitzbart, "Search for supersymmetric partners and anomalous couplings of the top quark with the CMS experiment". PhD thesis, Technische Universität Wien, 2019. doi:10.34726/hss.2019.67680.

[68] CMS Collaboration, "Differential cross section measurements for the production of top quark pairs and of additional jets using dilepton events from pp collisions at $\sqrt{s} = 13$ TeV", 2024. arXiv:2402.08486. Submitted to *JHEP*.

[69] CMS Collaboration, "Measurements of $t\bar{t}$ differential cross sections in proton-proton collisions at $\sqrt{s} = 13$ TeV using events containing two leptons", *JHEP* **02** (2019) 149, doi:10.1007/JHEP02(2019)149, arXiv:1811.06625.

[70] CMS Collaboration, "Measurement of differential cross sections for the production of top quark pairs and of additional jets in lepton+jets events from pp collisions at $\sqrt{s} = 13$ TeV", *Phys. Rev. D* **97** (2018) 112003, doi:10.1103/PhysRevD.97.112003, arXiv:1803.08856.

A The CMS Collaboration

Yerevan Physics Institute, Yerevan, Armenia
A. Hayrapetyan, A. Tumasyan[1]

Institut für Hochenergiephysik, Vienna, Austria
W. Adam, J.W. Andrejkovic, T. Bergauer, S. Chatterjee, K. Damanakis, M. Dragicevic, P.S. Hussain, M. Jeitler[2], N. Krammer, A. Li, D. Liko, I. Mikulec, J. Schieck[2], R. Schöfbeck, D. Schwarz, M. Sonawane, W. Waltenberger, C.-E. Wulz[2]

Universiteit Antwerpen, Antwerpen, Belgium
T. Janssen, T. Van Laer, P. Van Mechelen

Vrije Universiteit Brussel, Brussel, Belgium
N. Breugelmans, J. D'Hondt, S. Dansana, A. De Moor, M. Delcourt, F. Heyen, S. Lowette, I. Makarenko, D. Müller, S. Tavernier, M. Tytgat[3], G.P. Van Onsem, S. Van Putte, D. Vannerom

Université Libre de Bruxelles, Bruxelles, Belgium
B. Bilin, B. Clerbaux, A.K. Das, G. De Lentdecker, H. Evard, L. Favart, P. Gianneios, J. Jaramillo, A. Khalilzadeh, F.A. Khan, K. Lee, M. Mahdavikhorrami, A. Malara, S. Paredes, M.A. Shahzad, L. Thomas, M. Vanden Bemden, C. Vander Velde, P. Vanlaer

Ghent University, Ghent, Belgium
M. De Coen, D. Dobur, G. Gokbulut, Y. Hong, J. Knolle, L. Lambrecht, D. Marckx, K. Mota Amarilo, K. Skovpen, N. Van Den Bossche, J. van der Linden, L. Wezenbeek

Université Catholique de Louvain, Louvain-la-Neuve, Belgium
A. Benecke, A. Bethani, G. Bruno, C. Caputo, J. De Favereau De Jeneret, C. Delaere, I.S. Donertas, A. Giammanco, A.O. Guzel, Sa. Jain, V. Lemaitre, J. Lidrych, P. Mastrapasqua, T.T. Tran, S. Wertz

Centro Brasileiro de Pesquisas Fisicas, Rio de Janeiro, Brazil
G.A. Alves, M. Alves Gallo Pereira, E. Coelho, G. Correia Silva, C. Hensel, T. Menezes De Oliveira, C. Mora Herrera[4], A. Moraes, P. Rebello Teles, M. Soeiro, A. Vilela Pereira[4]

Universidade do Estado do Rio de Janeiro, Rio de Janeiro, Brazil
W.L. Aldá Júnior, M. Barroso Ferreira Filho, H. Brandao Malbouisson, W. Carvalho, J. Chinellato[5], E.M. Da Costa, G.G. Da Silveira[6], D. De Jesus Damiao, S. Fonseca De Souza, R. Gomes De Souza, T. Laux Kuhn, M. Macedo, J. Martins[7], L. Mundim, H. Nogima, J.P. Pinheiro, A. Santoro, A. Sznajder, M. Thiel

Universidade Estadual Paulista, Universidade Federal do ABC, São Paulo, Brazil
C.A. Bernardes[6], L. Calligaris, T.R. Fernandez Perez Tomei, E.M. Gregores, I. Maietto Silverio, P.G. Mercadante, S.F. Novaes, B. Orzari, Sandra S. Padula

Institute for Nuclear Research and Nuclear Energy, Bulgarian Academy of Sciences, Sofia, Bulgaria
A. Aleksandrov, G. Antchev, R. Hadjiiska, P. Iaydjiev, M. Misheva, M. Shopova, G. Sultanov

University of Sofia, Sofia, Bulgaria
A. Dimitrov, L. Litov, B. Pavlov, P. Petkov, A. Petrov, E. Shumka

Instituto De Alta Investigación, Universidad de Tarapacá, Casilla 7 D, Arica, Chile
S. Keshri, D. Laroze, S. Thakur

Beihang University, Beijing, China
T. Cheng, T. Javaid, L. Yuan

Department of Physics, Tsinghua University, Beijing, China
Z. Hu, Z. Liang, J. Liu, K. Yi[8,9]

Institute of High Energy Physics, Beijing, China
G.M. Chen[10], H.S. Chen[10], M. Chen[10], F. Iemmi, C.H. Jiang, A. Kapoor[11], H. Liao, Z.-A. Liu[12], R. Sharma[13], J.N. Song[12], J. Tao, C. Wang[10], J. Wang, Z. Wang[10], H. Zhang, J. Zhao

State Key Laboratory of Nuclear Physics and Technology, Peking University, Beijing, China
A. Agapitos, Y. Ban, S. Deng, B. Guo, C. Jiang, A. Levin, C. Li, Q. Li, Y. Mao, S. Qian, S.J. Qian, X. Qin, X. Sun, D. Wang, H. Yang, L. Zhang, Y. Zhao, C. Zhou

Guangdong Provincial Key Laboratory of Nuclear Science and Guangdong-Hong Kong Joint Laboratory of Quantum Matter, South China Normal University, Guangzhou, China
S. Yang

Sun Yat-Sen University, Guangzhou, China
Z. You

University of Science and Technology of China, Hefei, China
K. Jaffel, N. Lu

Nanjing Normal University, Nanjing, China
G. Bauer[14], B. Li, J. Zhang

Institute of Modern Physics and Key Laboratory of Nuclear Physics and Ion-beam Application (MOE) - Fudan University, Shanghai, China
X. Gao[15], Y. Li

Zhejiang University, Hangzhou, Zhejiang, China
Z. Lin, C. Lu, M. Xiao

Universidad de Los Andes, Bogota, Colombia
C. Avila, D.A. Barbosa Trujillo, A. Cabrera, C. Florez, J. Fraga, J.A. Reyes Vega

Universidad de Antioquia, Medellin, Colombia
F. Ramirez, C. Rendón, M. Rodriguez, A.A. Ruales Barbosa, J.D. Ruiz Alvarez

University of Split, Faculty of Electrical Engineering, Mechanical Engineering and Naval Architecture, Split, Croatia
D. Giljanovic, N. Godinovic, D. Lelas, A. Sculac

University of Split, Faculty of Science, Split, Croatia
M. Kovac, A. Petkovic, T. Sculac

Institute Rudjer Boskovic, Zagreb, Croatia
P. Bargassa, V. Brigljevic, B.K. Chitroda, D. Ferencek, K. Jakovcic, A. Starodumov[16], T. Susa

University of Cyprus, Nicosia, Cyprus
A. Attikis, K. Christoforou, A. Hadjiagapiou, C. Leonidou, J. Mousa, C. Nicolaou, L. Paizanos, F. Ptochos, P.A. Razis, H. Rykaczewski, H. Saka, A. Stepennov

Charles University, Prague, Czech Republic
M. Finger, M. Finger Jr., A. Kveton

Escuela Politecnica Nacional, Quito, Ecuador
E. Ayala

Universidad San Francisco de Quito, Quito, Ecuador
E. Carrera Jarrin

Academy of Scientific Research and Technology of the Arab Republic of Egypt, Egyptian Network of High Energy Physics, Cairo, Egypt
B. El-mahdy, S. Khalil[17], E. Salama[18,19]

Center for High Energy Physics (CHEP-FU), Fayoum University, El-Fayoum, Egypt
M. Abdullah Al-Mashad, M.A. Mahmoud

National Institute of Chemical Physics and Biophysics, Tallinn, Estonia
K. Ehataht, M. Kadastik, T. Lange, S. Nandan, C. Nielsen, J. Pata, M. Raidal, L. Tani, C. Veelken

Department of Physics, University of Helsinki, Helsinki, Finland
H. Kirschenmann, K. Osterberg, M. Voutilainen

Helsinki Institute of Physics, Helsinki, Finland
S. Bharthuar, N. Bin Norjoharuddeen, E. Brücken, F. Garcia, P. Inkaew, K.T.S. Kallonen, T. Lampén, K. Lassila-Perini, S. Lehti, T. Lindén, L. Martikainen, M. Myllymäki, M.m. Rantanen, H. Siikonen, J. Tuominiemi

Lappeenranta-Lahti University of Technology, Lappeenranta, Finland
P. Luukka, H. Petrow

IRFU, CEA, Université Paris-Saclay, Gif-sur-Yvette, France
M. Besancon, F. Couderc, M. Dejardin, D. Denegri, J.L. Faure, F. Ferri, S. Ganjour, P. Gras, G. Hamel de Monchenault, M. Kumar, V. Lohezic, J. Malcles, F. Orlandi, L. Portales, A. Rosowsky, M.Ö. Sahin, A. Savoy-Navarro[20], P. Simkina, M. Titov, M. Tornago

Laboratoire Leprince-Ringuet, CNRS/IN2P3, Ecole Polytechnique, Institut Polytechnique de Paris, Palaiseau, France
F. Beaudette, G. Boldrini, P. Busson, A. Cappati, C. Charlot, M. Chiusi, F. Damas, O. Davignon, A. De Wit, I.T. Ehle, B.A. Fontana Santos Alves, S. Ghosh, A. Gilbert, R. Granier de Cassagnac, A. Hakimi, B. Harikrishnan, L. Kalipoliti, G. Liu, M. Nguyen, C. Ochando, R. Salerno, J.B. Sauvan, Y. Sirois, L. Urda Gómez, E. Vernazza, A. Zabi, A. Zghiche

Université de Strasbourg, CNRS, IPHC UMR 7178, Strasbourg, France
J.-L. Agram[21], J. Andrea, D. Apparu, D. Bloch, J.-M. Brom, E.C. Chabert, C. Collard, S. Falke, U. Goerlach, R. Haeberle, A.-C. Le Bihan, M. Meena, O. Poncet, G. Saha, M.A. Sessini, P. Van Hove, P. Vaucelle

Centre de Calcul de l'Institut National de Physique Nucleaire et de Physique des Particules, CNRS/IN2P3, Villeurbanne, France

A. Di Florio

Institut de Physique des 2 Infinis de Lyon (IP2I), Villeurbanne, France
D. Amram, S. Beauceron, B. Blancon, G. Boudoul, N. Chanon, D. Contardo, P. Depasse, C. Dozen[22], H. El Mamouni, J. Fay, S. Gascon, M. Gouzevitch, C. Greenberg, G. Grenier, B. Ille, E. Jourd'huy, I.B. Laktineh, M. Lethuillier, L. Mirabito, S. Perries, A. Purohit, M. Vander Donckt, P. Verdier, J. Xiao

Georgian Technical University, Tbilisi, Georgia
I. Bagaturia[23], I. Lomidze, Z. Tsamalaidze[16]

RWTH Aachen University, I. Physikalisches Institut, Aachen, Germany
V. Botta, S. Consuegra Rodríguez, L. Feld, K. Klein, M. Lipinski, D. Meuser, A. Pauls, D. Pérez Adán, N. Röwert, M. Teroerde

RWTH Aachen University, III. Physikalisches Institut A, Aachen, Germany
S. Diekmann, A. Dodonova, N. Eich, D. Eliseev, F. Engelke, J. Erdmann, M. Erdmann, P. Fackeldey, B. Fischer, T. Hebbeker, K. Hoepfner, F. Ivone, A. Jung, M.y. Lee, F. Mausolf, M. Merschmeyer, A. Meyer, S. Mukherjee, D. Noll, F. Nowotny, A. Pozdnyakov, Y. Rath, W. Redjeb, F. Rehm, H. Reithler, V. Sarkisovi, A. Schmidt, C. Seth, A. Sharma, J.L. Spah, A. Stein, F. Torres Da Silva De Araujo[24], S. Wiedenbeck, S. Zaleski

RWTH Aachen University, III. Physikalisches Institut B, Aachen, Germany
C. Dziwok, G. Flügge, T. Kress, A. Nowack, O. Pooth, A. Stahl, T. Ziemons, A. Zotz

Deutsches Elektronen-Synchrotron, Hamburg, Germany
H. Aarup Petersen, M. Aldaya Martin, J. Alimena, S. Amoroso, Y. An, J. Bach, S. Baxter, M. Bayatmakou, H. Becerril Gonzalez, O. Behnke, A. Belvedere, F. Blekman[25], K. Borras[26], A. Campbell, A. Cardini, C. Cheng, F. Colombina, G. Eckerlin, D. Eckstein, L.I. Estevez Banos, O. Filatov, E. Gallo[25], A. Geiser, V. Guglielmi, M. Guthoff, A. Hinzmann, L. Jeppe, B. Kaech, M. Kasemann, C. Kleinwort, R. Kogler, M. Komm, D. Krücker, W. Lange, D. Leyva Pernia, K. Lipka[27], W. Lohmann[28], F. Lorkowski, R. Mankel, I.-A. Melzer-Pellmann, M. Mendizabal Morentin, A.B. Meyer, G. Milella, K. Moral Figueroa, A. Mussgiller, L.P. Nair, J. Niedziela, A. Nürnberg, Y. Otarid, J. Park, E. Ranken, A. Raspereza, D. Rastorguev, J. Rübenach, L. Rygaard, A. Saggio, M. Scham[29,26], S. Schnake[26], P. Schütze, C. Schwanenberger[25], D. Selivanova, K. Sharko, M. Shchedrolosiev, D. Stafford, F. Vazzoler, A. Ventura Barroso, R. Walsh, D. Wang, Q. Wang, Y. Wen, K. Wichmann, L. Wiens[26], C. Wissing, Y. Yang, A. Zimermmane Castro Santos

University of Hamburg, Hamburg, Germany
A. Albrecht, S. Albrecht, M. Antonello, S. Bein, L. Benato, S. Bollweg, M. Bonanomi, P. Connor, K. El Morabit, Y. Fischer, E. Garutti, A. Grohsjean, J. Haller, H.R. Jabusch, G. Kasieczka, P. Keicher, R. Klanner, W. Korcari, T. Kramer, C.c. Kuo, V. Kutzner, F. Labe, J. Lange, A. Lobanov, C. Matthies, L. Moureaux, M. Mrowietz, A. Nigamova, Y. Nissan, A. Paasch, K.J. Pena Rodriguez, T. Quadfasel, B. Raciti, M. Rieger, D. Savoiu, J. Schindler, P. Schleper, M. Schröder, J. Schwandt, M. Sommerhalder, H. Stadie, G. Steinbrück, A. Tews, M. Wolf

Karlsruher Institut fuer Technologie, Karlsruhe, Germany
S. Brommer, M. Burkart, E. Butz, T. Chwalek, A. Dierlamm, A. Droll, U. Elicabuk, N. Faltermann, M. Giffels, A. Gottmann, F. Hartmann[30], R. Hofsaess, M. Horzela, U. Husemann, J. Kieseler, M. Klute, R. Koppenhöfer, J.M. Lawhorn, M. Link, A. Lintuluoto, S. Maier, S. Mitra, M. Mormile, Th. Müller, M. Neukum, M. Oh, E. Pfeffer, M. Presilla, G. Quast, K. Rabbertz, B. Regnery, N. Shadskiy, I. Shvetsov, H.J. Simonis, L. Sowa, L. Stockmeier, K. Tauqeer, M. Toms, N. Trevisani, R.F. Von Cube, M. Wassmer, S. Wieland, F. Wittig, R. Wolf, X. Zuo

Institute of Nuclear and Particle Physics (INPP), NCSR Demokritos, Aghia Paraskevi, Greece
G. Anagnostou, G. Daskalakis, A. Kyriakis, A. Papadopoulos[30], A. Stakia

National and Kapodistrian University of Athens, Athens, Greece
P. Kontaxakis, G. Melachroinos, Z. Painesis, I. Papavergou, I. Paraskevas, N. Saoulidou, K. Theofilatos, E. Tziaferi, K. Vellidis, I. Zisopoulos

National Technical University of Athens, Athens, Greece
G. Bakas, T. Chatzistavrou, G. Karapostoli, K. Kousouris, I. Papakrivopoulos, E. Siamarkou, G. Tsipolitis, A. Zacharopoulou

University of Ioánnina, Ioánnina, Greece
K. Adamidis, I. Bestintzanos, I. Evangelou, C. Foudas, C. Kamtsikis, P. Katsoulis, P. Kokkas, P.G. Kosmoglou Kioseoglou, N. Manthos, I. Papadopoulos, J. Strologas

HUN-REN Wigner Research Centre for Physics, Budapest, Hungary
C. Hajdu, D. Horvath[31,32], K. Márton, A.J. Rádl[33], F. Sikler, V. Veszpremi

MTA-ELTE Lendület CMS Particle and Nuclear Physics Group, Eötvös Loránd University, Budapest, Hungary
M. Csanád, K. Farkas, A. Fehérkuti[34], M.M.A. Gadallah[35], Á. Kadlecsik, P. Major, G. Pásztor, G.I. Veres

Faculty of Informatics, University of Debrecen, Debrecen, Hungary
B. Ujvari, G. Zilizi

HUN-REN ATOMKI - Institute of Nuclear Research, Debrecen, Hungary
G. Bencze, S. Czellar, J. Molnar, Z. Szillasi

Karoly Robert Campus, MATE Institute of Technology, Gyongyos, Hungary
T. Csorgo[34], F. Nemes[34], T. Novak

Panjab University, Chandigarh, India
S. Bansal, S.B. Beri, V. Bhatnagar, G. Chaudhary, S. Chauhan, N. Dhingra[36], A. Kaur, A. Kaur, H. Kaur, M. Kaur, S. Kumar, K. Sandeep, T. Sheokand, J.B. Singh, A. Singla

University of Delhi, Delhi, India
A. Ahmed, A. Bhardwaj, A. Chhetri, B.C. Choudhary, A. Kumar, A. Kumar, M. Naimuddin, K. Ranjan, M.K. Saini, S. Saumya

Saha Institute of Nuclear Physics, HBNI, Kolkata, India
S. Baradia, S. Barman[37], S. Bhattacharya, S. Das Gupta, S. Dutta, S. Dutta, S. Sarkar

Indian Institute of Technology Madras, Madras, India
M.M. Ameen, P.K. Behera, S.C. Behera, S. Chatterjee, G. Dash, P. Jana,

P. Kalbhor, S. Kamble, J.R. Komaragiri[38], D. Kumar[38], B. Parida, P.R. Pujahari, N.R. Saha, A. Sharma, A.K. Sikdar, R.K. Singh, P. Verma, S. Verma, A. Vijay

Tata Institute of Fundamental Research-A, Mumbai, India
S. Dugad, G.B. Mohanty, M. Shelake, P. Suryadevara

Tata Institute of Fundamental Research-B, Mumbai, India
A. Bala, S. Banerjee, R.M. Chatterjee, M. Guchait, Sh. Jain, A. Jaiswal, S. Kumar, G. Majumder, K. Mazumdar, S. Parolia, A. Thachayath

National Institute of Science Education and Research, An OCC of Homi Bhabha National Institute, Bhubaneswar, Odisha, India
S. Bahinipati[39], C. Kar, D. Maity[40], P. Mal, T. Mishra, V.K. Muraleedharan Nair Bindhu[40], K. Naskar[40], A. Nayak[40], S. Nayak, K. Pal, P. Sadangi, S.K. Swain, S. Varghese[40], D. Vats[40]

Indian Institute of Science Education and Research (IISER), Pune, India
S. Acharya[41], A. Alpana, S. Dube, B. Gomber[41], P. Hazarika, B. Kansal, A. Laha, B. Sahu[41], S. Sharma, K.Y. Vaish

Isfahan University of Technology, Isfahan, Iran
H. Bakhshiansohi[42], A. Jafari[43], M. Zeinali[44]

Institute for Research in Fundamental Sciences (IPM), Tehran, Iran
S. Bashiri, S. Chenarani[45], S.M. Etesami, Y. Hosseini, M. Khakzad, E. Khazaie[46], M. Mohammadi Najafabadi, S. Tizchang[47]

University College Dublin, Dublin, Ireland
M. Felcini, M. Grunewald

INFN Sezione di Bari[a], Università di Bari[b], Politecnico di Bari[c], Bari, Italy
M. Abbrescia[a,b], A. Colaleo[a,b], D. Creanza[a,c], B. D'Anzi[a,b], N. De Filippis[a,c], M. De Palma[a,b], W. Elmetenawee[a,b,48], L. Fiore[a], G. Iaselli[a,c], L. Longo[a], M. Louka[a,b], G. Maggi[a,c], M. Maggi[a], I. Margjeka[a], V. Mastrapasqua[a,b], S. My[a,b], S. Nuzzo[a,b], A. Pellecchia[a,b], A. Pompili[a,b], G. Pugliese[a,c], R. Radogna[a,b], D. Ramos[a], A. Ranieri[a], L. Silvestris[a], F.M. Simone[a,c], Ü. Sözbilir[a], A. Stamerra[a,b], D. Troiano[a,b], R. Venditti[a,b], P. Verwilligen[a], A. Zaza[a,b]

INFN Sezione di Bologna[a], Università di Bologna[b], Bologna, Italy
G. Abbiendi[a], C. Battilana[a,b], D. Bonacorsi[a,b], P. Capiluppi[a,b], A. Castro[†a,b], F.R. Cavallo[a], M. Cuffiani[a,b], G.M. Dallavalle[a], T. Diotalevi[a,b], F. Fabbri[a], A. Fanfani[a,b], D. Fasanella[a], P. Giacomelli[a], L. Giommi[a,b], C. Grandi[a], L. Guiducci[a,b], S. Lo Meo[a,49], M. Lorusso[a,b], L. Lunerti[a], S. Marcellini[a], G. Masetti[a], F.L. Navarria[a,b], G. Paggi[a,b], A. Perrotta[a], F. Primavera[a,b], A.M. Rossi[a,b], S. Rossi Tisbeni[a,b], T. Rovelli[a,b], G.P. Siroli[a,b]

INFN Sezione di Catania[a], Università di Catania[b], Catania, Italy
S. Costa[a,b,50], A. Di Mattia[a], A. Lapertosa[a], R. Potenza[a,b], A. Tricomi[a,b,50], C. Tuve[a,b]

INFN Sezione di Firenze[a], Università di Firenze[b], Firenze, Italy
P. Assiouras[a], G. Barbagli[a], G. Bardelli[a,b], B. Camaiani[a,b], A. Cassese[a], R. Ceccarelli[a], V. Ciulli[a,b], C. Civinini[a], R. D'Alessandro[a,b], E. Focardi[a,b], T. Kello[a], G. Latino[a,b], P. Lenzi[a,b], M. Lizzo[a], M. Meschini[a], S. Paoletti[a], A. Papanastassiou[a,b], G. Sguazzoni[a], L. Viliani[a]

INFN Laboratori Nazionali di Frascati, Frascati, Italy
L. Benussi, S. Bianco, S. Meola[51], D. Piccolo

INFN Sezione di Genova[a], Università di Genova[b], Genova, Italy
P. Chatagnon[a], F. Ferro[a], E. Robutti[a], S. Tosi[a,b]

INFN Sezione di Milano-Bicocca[a], Università di Milano-Bicocca[b], Milano, Italy
A. Benaglia[a], F. Brivio[a], F. Cetorelli[a,b], F. De Guio[a,b], M.E. Dinardo[a,b], P. Dini[a], S. Gennai[a], R. Gerosa[a,b], A. Ghezzi[a,b], P. Govoni[a,b], L. Guzzi[a], M.T. Lucchini[a,b], M. Malberti[a], S. Malvezzi[a], A. Massironi[a], D. Menasce[a], L. Moroni[a], M. Paganoni[a,b], S. Palluotto[a,b], D. Pedrini[a], A. Perego[a,b], B.S. Pinolini[a], G. Pizzati[a,b], S. Ragazzi[a,b], T. Tabarelli de Fatis[a,b]

INFN Sezione di Napoli[a], Università di Napoli 'Federico II'[b], Napoli, Italy; Università della Basilicata[c], Potenza, Italy; Scuola Superiore Meridionale (SSM)[d], Napoli, Italy
S. Buontempo[a], A. Cagnotta[a,b], F. Carnevali[a,b], N. Cavallo[a,c], F. Fabozzi[a,c], A.O.M. Iorio[a,b], L. Lista[a,b,52], P. Paolucci[a,30], B. Rossi[a]

INFN Sezione di Padova[a], Università di Padova[b], Padova, Italy; Università di Trento[c], Trento, Italy
R. Ardino[a], P. Azzi[a], N. Bacchetta[a,53], M. Bellato[a], M. Benettoni[a], D. Bisello[a,b], P. Bortignon[a], G. Bortolato[a,b], A. Bragagnolo[a,b], A.C.M. Bulla[a], R. Carlin[a,b], P. Checchia[a], T. Dorigo[a], U. Gasparini[a,b], S. Giorgetti[a], E. Lusiani[a], M. Margoni[a,b], M. Migliorini[a,b], J. Pazzini[a,b], P. Ronchese[a,b], R. Rossin[a,b], F. Simonetto[a,b], M. Tosi[a,b], A. Triossi[a,b], S. Ventura[a], M. Zanetti[a,b], P. Zotto[a,b], A. Zucchetta[a,b], G. Zumerle[a,b]

INFN Sezione di Pavia[a], Università di Pavia[b], Pavia, Italy
C. Aimè[a], A. Braghieri[a], S. Calzaferri[a], D. Fiorina[a], P. Montagna[a,b], V. Re[a], C. Riccardi[a,b], P. Salvini[a], I. Vai[a,b], P. Vitulo[a,b]

INFN Sezione di Perugia[a], Università di Perugia[b], Perugia, Italy
S. Ajmal[a,b], M.E. Ascioti[a,b], G.M. Bilei[a], C. Carrivale[a,b], D. Ciangottini[a,b], L. Fanò[a,b], M. Magherini[a,b], V. Mariani[a,b], M. Menichelli[a], F. Moscatelli[a,54], A. Rossi[a,b], A. Santocchia[a,b], D. Spiga[a], T. Tedeschi[a,b]

INFN Sezione di Pisa[a], Università di Pisa[b], Scuola Normale Superiore di Pisa[c], Pisa, Italy; Università di Siena[d], Siena, Italy
C.A. Alexe[a,c], P. Asenov[a,b], P. Azzurri[a], G. Bagliesi[a], R. Bhattacharya[a], L. Bianchini[a,b], T. Boccali[a], E. Bossini[a], D. Bruschini[a,c], R. Castaldi[a], M.A. Ciocci[a,b], M. Cipriani[a,b], V. D'Amante[a,d], R. Dell'Orso[a], S. Donato[a], A. Giassi[a], F. Ligabue[a,c], A.C. Marini[a], D. Matos Figueiredo[a], A. Messineo[a,b], S. Mishra[a], M. Musich[a,b], F. Palla[a], A. Rizzi[a,b], G. Rolandi[a,c], S. Roy Chowdhury[a], T. Sarkar[a], A. Scribano[a], P. Spagnolo[a], R. Tenchini[a], G. Tonelli[a,b], N. Turini[a,d], F. Vaselli[a,c], A. Venturi[a], P.G. Verdini[a]

INFN Sezione di Roma[a], Sapienza Università di Roma[b], Roma, Italy
C. Baldenegro Barrera[a,b], P. Barria[a], C. Basile[a,b], F. Cavallari[a], L. Cunqueiro Mendez[a,b], D. Del Re[a,b], E. Di Marco[a,b], M. Diemoz[a], F. Errico[a,b], E. Longo[a,b], J. Mijuskovic[a,b], G. Organtini[a,b], F. Pandolfi[a], R. Paramatti[a,b], C. Quaranta[a,b], S. Rahatlou[a,b], C. Rovelli[a], F. Santanastasio[a,b], L. Soffi[a]

INFN Sezione di Torino[a], Università di Torino[b], Torino, Italy; Università del Piemonte Orientale[c], Novara, Italy

N. Amapane[a,b], R. Arcidiacono[a,c], S. Argiro[a,b], M. Arneodo[a,c], N. Bartosik[a], R. Bellan[a,b], A. Bellora[a,b], C. Biino[a], C. Borca[a,b], N. Cartiglia[a], M. Costa[a,b], R. Covarelli[a,b], N. Demaria[a], L. Finco[a], M. Grippo[a,b], B. Kiani[a,b], F. Legger[a], F. Luongo[a,b], C. Mariotti[a], L. Markovic[a,b], S. Maselli[a], A. Mecca[a,b], L. Menzio[a,b], P. Meridiani[a], E. Migliore[a,b], M. Monteno[a], R. Mulargia[a], M.M. Obertino[a,b], G. Ortona[a], L. Pacher[a,b], N. Pastrone[a], M. Pelliccioni[a], M. Ruspa[a,c], F. Siviero[a,b], V. Sola[a,b], A. Solano[a,b], A. Staiano[a], C. Tarricone[a,b], D. Trocino[a], G. Umoret[a,b], R. White[a,b]

INFN Sezione di Trieste[a], Università di Trieste[b], Trieste, Italy
J. Babbar[a,b], S. Belforte[a], V. Candelise[a,b], M. Casarsa[a], F. Cossutti[a], K. De Leo[a], G. Della Ricca[a,b]

Kyungpook National University, Daegu, Korea
S. Dogra, J. Hong, B. Kim, J. Kim, D. Lee, H. Lee, S.W. Lee, C.S. Moon, Y.D. Oh, M.S. Ryu, S. Sekmen, B. Tae, Y.C. Yang

Department of Mathematics and Physics - GWNU, Gangneung, Korea
M.S. Kim

Chonnam National University, Institute for Universe and Elementary Particles, Kwangju, Korea
G. Bak, P. Gwak, H. Kim, D.H. Moon

Hanyang University, Seoul, Korea
E. Asilar, J. Choi, D. Kim, T.J. Kim, J.A. Merlin, Y. Ryou

Korea University, Seoul, Korea
S. Choi, S. Han, B. Hong, K. Lee, K.S. Lee, S. Lee, J. Yoo

Kyung Hee University, Department of Physics, Seoul, Korea
J. Goh, S. Yang

Sejong University, Seoul, Korea
H. S. Kim, Y. Kim, S. Lee

Seoul National University, Seoul, Korea
J. Almond, J.H. Bhyun, J. Choi, J. Choi, W. Jun, J. Kim, Y.W. Kim, S. Ko, H. Kwon, H. Lee, J. Lee, J. Lee, B.H. Oh, S.B. Oh, H. Seo, U.K. Yang, I. Yoon

University of Seoul, Seoul, Korea
W. Jang, D.Y. Kang, Y. Kang, S. Kim, B. Ko, J.S.H. Lee, Y. Lee, I.C. Park, Y. Roh, I.J. Watson

Yonsei University, Department of Physics, Seoul, Korea
S. Ha, H.D. Yoo

Sungkyunkwan University, Suwon, Korea
M. Choi, M.R. Kim, H. Lee, Y. Lee, I. Yu

College of Engineering and Technology, American University of the Middle East (AUM), Dasman, Kuwait
T. Beyrouthy, Y. Gharbia

Kuwait University - College of Science - Department of Physics, Safat, Kuwait
F. Alazemi

Riga Technical University, Riga, Latvia
K. Dreimanis, A. Gaile, C. Munoz Diaz, D. Osite, G. Pikurs, A. Potrebko, M. Seidel, D. Sidiropoulos Kontos

University of Latvia (LU), Riga, Latvia
N.R. Strautnieks

Vilnius University, Vilnius, Lithuania
M. Ambrozas, A. Juodagalvis, A. Rinkevicius, G. Tamulaitis

National Centre for Particle Physics, Universiti Malaya, Kuala Lumpur, Malaysia
I. Yusuff[55], Z. Zolkapli

Universidad de Sonora (UNISON), Hermosillo, Mexico
J.F. Benitez, A. Castaneda Hernandez, H.A. Encinas Acosta, L.G. Gallegos Maríñez, M. León Coello, J.A. Murillo Quijada, A. Sehrawat, L. Valencia Palomo

Centro de Investigacion y de Estudios Avanzados del IPN, Mexico City, Mexico
G. Ayala, H. Castilla-Valdez, H. Crotte Ledesma, E. De La Cruz-Burelo, I. Heredia-De La Cruz[56], R. Lopez-Fernandez, J. Mejia Guisao, C.A. Mondragon Herrera, A. Sánchez Hernández

Universidad Iberoamericana, Mexico City, Mexico
C. Oropeza Barrera, D.L. Ramirez Guadarrama, M. Ramírez García

Benemerita Universidad Autonoma de Puebla, Puebla, Mexico
I. Bautista, I. Pedraza, H.A. Salazar Ibarguen, C. Uribe Estrada

University of Montenegro, Podgorica, Montenegro
I. Bubanja, N. Raicevic

University of Canterbury, Christchurch, New Zealand
P.H. Butler

National Centre for Physics, Quaid-I-Azam University, Islamabad, Pakistan
A. Ahmad, M.I. Asghar, A. Awais, M.I.M. Awan, H.R. Hoorani, W.A. Khan

AGH University of Krakow, Faculty of Computer Science, Electronics and Telecommunications, Krakow, Poland
V. Avati, L. Grzanka, M. Malawski

National Centre for Nuclear Research, Swierk, Poland
H. Bialkowska, M. Bluj, M. Górski, M. Kazana, M. Szleper, P. Zalewski

Institute of Experimental Physics, Faculty of Physics, University of Warsaw, Warsaw, Poland
K. Bunkowski, K. Doroba, A. Kalinowski, M. Konecki, J. Krolikowski, A. Muhammad

Warsaw University of Technology, Warsaw, Poland
K. Pozniak, W. Zabolotny

Laboratório de Instrumentação e Física Experimental de Partículas, Lisboa, Portugal
M. Araujo, D. Bastos, C. Beirão Da Cruz E Silva, A. Boletti, M. Bozzo, T. Camporesi, G. Da Molin, P. Faccioli, M. Gallinaro, J. Hollar, N. Leonardo, G.B. Marozzo, T. Niknejad, A. Petrilli, M. Pisano, J. Seixas, J. Varela, J.W. Wulff

Faculty of Physics, University of Belgrade, Belgrade, Serbia

P. Adzic, P. Milenovic

VINCA Institute of Nuclear Sciences, University of Belgrade, Belgrade, Serbia
D. Devetak, M. Dordevic, J. Milosevic, V. Rekovic

Centro de Investigaciones Energéticas Medioambientales y Tecnológicas (CIEMAT), Madrid, Spain
J. Alcaraz Maestre, Cristina F. Bedoya, J.A. Brochero Cifuentes, Oliver M. Carretero, M. Cepeda, M. Cerrada, N. Colino, B. De La Cruz, A. Delgado Peris, A. Escalante Del Valle, D. Fernández Del Val, J.P. Fernández Ramos, J. Flix, M.C. Fouz, O. Gonzalez Lopez, S. Goy Lopez, J.M. Hernandez, M.I. Josa, J. Llorente Merino, E. Martin Viscasillas, D. Moran, C. M. Morcillo Perez, Á. Navarro Tobar, C. Perez Dengra, A. Pérez-Calero Yzquierdo, J. Puerta Pelayo, I. Redondo, S. Sánchez Navas, J. Sastre, J. Vazquez Escobar

Universidad Autónoma de Madrid, Madrid, Spain
J.F. de Trocóniz

Universidad de Oviedo, Instituto Universitario de Ciencias y Tecnologías Espaciales de Asturias (ICTEA), Oviedo, Spain
B. Alvarez Gonzalez, J. Cuevas, J. Fernandez Menendez, S. Folgueras, I. Gonzalez Caballero, J.R. González Fernández, P. Leguina, E. Palencia Cortezon, J. Prado Pico, C. Ramón Álvarez, V. Rodríguez Bouza, A. Soto Rodríguez, A. Trapote, C. Vico Villalba, P. Vischia

Instituto de Física de Cantabria (IFCA), CSIC-Universidad de Cantabria, Santander, Spain
S. Bhowmik, S. Blanco Fernández, I.J. Cabrillo, A. Calderon, J. Duarte Campderros, M. Fernandez, G. Gomez, C. Lasaosa García, R. Lopez Ruiz, C. Martinez Rivero, P. Martinez Ruiz del Arbol, F. Matorras, P. Matorras Cuevas, E. Navarrete Ramos, J. Piedra Gomez, L. Scodellaro, I. Vila, J.M. Vizan Garcia

University of Colombo, Colombo, Sri Lanka
B. Kailasapathy[57], D.D.C. Wickramarathna

University of Ruhuna, Department of Physics, Matara, Sri Lanka
W.G.D. Dharmaratna[58], K. Liyanage, N. Perera

CERN, European Organization for Nuclear Research, Geneva, Switzerland
D. Abbaneo, C. Amendola, E. Auffray, G. Auzinger, J. Baechler, D. Barney, A. Bermúdez Martínez, M. Bianco, A.A. Bin Anuar, A. Bocci, L. Borgonovi, C. Botta, E. Brondolin, C. Caillol, G. Cerminara, N. Chernyavskaya, D. d'Enterria, A. Dabrowski, A. David, A. De Roeck, M.M. Defranchis, M. Deile, M. Dobson, G. Franzoni, W. Funk, S. Giani, D. Gigi, K. Gill, F. Glege, J. Hegeman, J.K. Heikkilä, B. Huber, V. Innocente, T. James, P. Janot, O. Kaluzinska, O. Karacheban[28], S. Laurila, P. Lecoq, E. Leutgeb, C. Lourenço, L. Malgeri, M. Mannelli, M. Matthewman, A. Mehta, F. Meijers, S. Mersi, E. Meschi, V. Milosevic, F. Monti, F. Moortgat, M. Mulders, I. Neutelings, S. Orfanelli, F. Pantaleo, G. Petrucciani, A. Pfeiffer, M. Pierini, H. Qu, D. Rabady, B. Ribeiro Lopes, M. Rovere, H. Sakulin, S. Sanchez Cruz, S. Scarfi, C. Schwick, M. Selvaggi, A. Sharma, K. Shchelina, P. Silva, P. Sphicas[59], A.G. Stahl Leiton, A. Steen, S. Summers, D. Treille, P. Tropea, D. Walter, J. Wanczyk[60], J. Wang, K.A. Wozniak[61], S. Wuchterl, P. Zehetner, P. Zejdl, W.D. Zeuner

Paul Scherrer Institut, Villigen, Switzerland

T. Bevilacqua[62], L. Caminada[62], A. Ebrahimi, W. Erdmann, R. Horisberger, Q. Ingram, H.C. Kaestli, D. Kotlinski, C. Lange, M. Missiroli[62], L. Noehte[62], T. Rohe, A. Samalan

ETH Zurich - Institute for Particle Physics and Astrophysics (IPA), Zurich, Switzerland
T.K. Aarrestad, K. Androsov[60], M. Backhaus, G. Bonomelli, A. Calandri, C. Cazzaniga, K. Datta, P. De Bryas Dexmiers D'archiac[60], A. De Cosa, G. Dissertori, M. Dittmar, M. Donegà, F. Eble, M. Galli, K. Gedia, F. Glessgen, C. Grab, N. Härringer, T.G. Harte, D. Hits, W. Lustermann, A.-M. Lyon, R.A. Manzoni, M. Marchegiani, L. Marchese, C. Martin Perez, A. Mascellani[60], F. Nessi-Tedaldi, F. Pauss, V. Perovic, S. Pigazzini, B. Ristic, F. Riti, R. Seidita, J. Steggemann[60], A. Tarabini, D. Valsecchi, R. Wallny

Universität Zürich, Zurich, Switzerland
C. Amsler[63], P. Bärtschi, M.F. Canelli, K. Cormier, M. Huwiler, W. Jin, A. Jofrehei, B. Kilminster, S. Leontsinis, S.P. Liechti, A. Macchiolo, P. Meiring, F. Meng, U. Molinatti, J. Motta, A. Reimers, P. Robmann, M. Senger, E. Shokr, F. Stäger, R. Tramontano

National Central University, Chung-Li, Taiwan
C. Adloff[64], D. Bhowmik, C.M. Kuo, W. Lin, P.K. Rout, P.C. Tiwari[38], S.S. Yu

National Taiwan University (NTU), Taipei, Taiwan
L. Ceard, K.F. Chen, P.s. Chen, Z.g. Chen, A. De Iorio, W.-S. Hou, T.h. Hsu, Y.w. Kao, S. Karmakar, G. Kole, Y.y. Li, R.-S. Lu, E. Paganis, X.f. Su, J. Thomas-Wilsker, L.s. Tsai, D. Tsionou, H.y. Wu, E. Yazgan

High Energy Physics Research Unit, Department of Physics, Faculty of Science, Chulalongkorn University, Bangkok, Thailand
C. Asawatangtrakuldee, N. Srimanobhas, V. Wachirapusitanand

Çukurova University, Physics Department, Science and Art Faculty, Adana, Turkey
D. Agyel, F. Boran, F. Dolek, I. Dumanoglu[65], E. Eskut, Y. Guler[66], E. Gurpinar Guler[66], C. Isik, O. Kara, A. Kayis Topaksu, U. Kiminsu, G. Onengut, K. Ozdemir[67], A. Polatoz, B. Tali[68], U.G. Tok, S. Turkcapar, E. Uslan, I.S. Zorbakir

Middle East Technical University, Physics Department, Ankara, Turkey
G. Sokmen, M. Yalvac[69]

Bogazici University, Istanbul, Turkey
B. Akgun, I.O. Atakisi, E. Gülmez, M. Kaya[70], O. Kaya[71], S. Tekten[72]

Istanbul Technical University, Istanbul, Turkey
A. Cakir, K. Cankocak[65,73], G.G. Dincer[65], Y. Komurcu, S. Sen[74]

Istanbul University, Istanbul, Turkey
O. Aydilek[75], B. Hacisahinoglu, I. Hos[76], B. Kaynak, S. Ozkorucuklu, O. Potok, H. Sert, C. Simsek, C. Zorbilmez

Yildiz Technical University, Istanbul, Turkey
S. Cerci[68], B. Isildak[77], D. Sunar Cerci, T. Yetkin

Institute for Scintillation Materials of National Academy of Science of Ukraine, Kharkiv, Ukraine

A. Boyaryntsev, B. Grynyov

National Science Centre, Kharkiv Institute of Physics and Technology, Kharkiv, Ukraine
L. Levchuk

University of Bristol, Bristol, United Kingdom
D. Anthony, J.J. Brooke, A. Bundock, F. Bury, E. Clement, D. Cussans, H. Flacher, M. Glowacki, J. Goldstein, H.F. Heath, M.-L. Holmberg, L. Kreczko, S. Paramesvaran, L. Robertshaw, S. Seif El Nasr-Storey, V.J. Smith, N. Stylianou[78], K. Walkingshaw Pass

Rutherford Appleton Laboratory, Didcot, United Kingdom
A.H. Ball, K.W. Bell, A. Belyaev[79], C. Brew, R.M. Brown, D.J.A. Cockerill, C. Cooke, A. Elliot, K.V. Ellis, K. Harder, S. Harper, J. Linacre, K. Manolopoulos, D.M. Newbold, E. Olaiya, D. Petyt, T. Reis, A.R. Sahasransu, G. Salvi, T. Schuh, C.H. Shepherd-Themistocleous, I.R. Tomalin, K.C. Whalen, T. Williams

Imperial College, London, United Kingdom
I. Andreou, R. Bainbridge, P. Bloch, C.E. Brown, O. Buchmuller, V. Cacchio, C.A. Carrillo Montoya, G.S. Chahal[80], D. Colling, J.S. Dancu, I. Das, P. Dauncey, G. Davies, J. Davies, M. Della Negra, S. Fayer, G. Fedi, G. Hall, M.H. Hassanshahi, A. Howard, G. Iles, C.R. Knight, J. Langford, J. León Holgado, L. Lyons, A.-M. Magnan, B. Maier, S. Mallios, M. Mieskolainen, J. Nash[81], M. Pesaresi, P.B. Pradeep, B.C. Radburn-Smith, A. Richards, A. Rose, K. Savva, C. Seez, R. Shukla, A. Tapper, K. Uchida, G.P. Uttley, L.H. Vage, T. Virdee[30], M. Vojinovic, N. Wardle, D. Winterbottom

Brunel University, Uxbridge, United Kingdom
J.E. Cole, A. Khan, P. Kyberd, I.D. Reid

Baylor University, Waco, Texas, USA
S. Abdullin, A. Brinkerhoff, E. Collins, M.R. Darwish[82], J. Dittmann, K. Hatakeyama, J. Hiltbrand, B. McMaster, J. Samudio, S. Sawant, C. Sutantawibul, J. Wilson

Catholic University of America, Washington, DC, USA
R. Bartek, A. Dominguez, C. Huerta Escamilla, A.E. Simsek, R. Uniyal, A.M. Vargas Hernandez

The University of Alabama, Tuscaloosa, Alabama, USA
B. Bam, A. Buchot Perraguin, R. Chudasama, S.I. Cooper, C. Crovella, S.V. Gleyzer, E. Pearson, C.U. Perez, P. Rumerio[83], E. Usai, R. Yi

Boston University, Boston, Massachusetts, USA
A. Akpinar, C. Cosby, G. De Castro, Z. Demiragli, C. Erice, C. Fangmeier, C. Fernandez Madrazo, E. Fontanesi, D. Gastler, F. Golf, S. Jeon, J. O'cain, I. Reed, J. Rohlf, K. Salyer, D. Sperka, D. Spitzbart, I. Suarez, A. Tsatsos, A.G. Zecchinelli

Brown University, Providence, Rhode Island, USA
G. Benelli, D. Cutts, L. Gouskos, M. Hadley, U. Heintz, J.M. Hogan[84], T. Kwon, G. Landsberg, K.T. Lau, D. Li, J. Luo, S. Mondal, N. Pervan, T. Russell, S. Sagir[85], X. Shen, F. Simpson, M. Stamenkovic, N. Venkatasubramanian, X. Yan

University of California, Davis, Davis, California, USA
S. Abbott, C. Brainerd, R. Breedon, H. Cai, M. Calderon De La Barca Sanchez, M. Chertok, M. Citron, J. Conway, P.T. Cox, R. Erbacher, F. Jensen, O. Kukral, G. Mocellin, M. Mulhearn, S. Ostrom, W. Wei, S. Yoo, F. Zhang

University of California, Los Angeles, California, USA
M. Bachtis, R. Cousins, A. Datta, G. Flores Avila, J. Hauser, M. Ignatenko, M.A. Iqbal, T. Lam, E. Manca, A. Nunez Del Prado, D. Saltzberg, V. Valuev

University of California, Riverside, Riverside, California, USA
R. Clare, J.W. Gary, M. Gordon, G. Hanson, W. Si

University of California, San Diego, La Jolla, California, USA
A. Aportela, A. Arora, J.G. Branson, S. Cittolin, S. Cooperstein, D. Diaz, J. Duarte, L. Giannini, Y. Gu, J. Guiang, R. Kansal, V. Krutelyov, R. Lee, J. Letts, M. Masciovecchio, F. Mokhtar, S. Mukherjee, M. Pieri, M. Quinnan, B.V. Sathia Narayanan, V. Sharma, M. Tadel, E. Vourliotis, F. Würthwein, Y. Xiang, A. Yagil

University of California, Santa Barbara - Department of Physics, Santa Barbara, California, USA
A. Barzdukas, L. Brennan, C. Campagnari, K. Downham, C. Grieco, J. Incandela, J. Kim, A.J. Li, P. Masterson, H. Mei, J. Richman, S.N. Santpur, U. Sarica, R. Schmitz, F. Setti, J. Sheplock, D. Stuart, T.Á. Vámi, S. Wang, D. Zhang

California Institute of Technology, Pasadena, California, USA
S. Bhattacharya, A. Bornheim, O. Cerri, A. Latorre, J. Mao, H.B. Newman, G. Reales Gutiérrez, M. Spiropulu, J.R. Vlimant, C. Wang, S. Xie, R.Y. Zhu

Carnegie Mellon University, Pittsburgh, Pennsylvania, USA
J. Alison, S. An, P. Bryant, M. Cremonesi, V. Dutta, T. Ferguson, T.A. Gómez Espinosa, A. Harilal, A. Kallil Tharayil, C. Liu, T. Mudholkar, S. Murthy, P. Palit, K. Park, M. Paulini, A. Roberts, A. Sanchez, W. Terrill

University of Colorado Boulder, Boulder, Colorado, USA
J.P. Cumalat, W.T. Ford, A. Hart, A. Hassani, G. Karathanasis, N. Manganelli, J. Pearkes, C. Savard, N. Schonbeck, K. Stenson, K.A. Ulmer, S.R. Wagner, N. Zipper, D. Zuolo

Cornell University, Ithaca, New York, USA
J. Alexander, S. Bright-Thonney, X. Chen, D.J. Cranshaw, J. Fan, X. Fan, S. Hogan, P. Kotamnives, J. Monroy, M. Oshiro, J.R. Patterson, M. Reid, A. Ryd, J. Thom, P. Wittich, R. Zou

Fermi National Accelerator Laboratory, Batavia, Illinois, USA
M. Albrow, M. Alyari, O. Amram, G. Apollinari, A. Apresyan, L.A.T. Bauerdick, D. Berry, J. Berryhill, P.C. Bhat, K. Burkett, J.N. Butler, A. Canepa, G.B. Cerati, H.W.K. Cheung, F. Chlebana, G. Cummings, J. Dickinson, I. Dutta, V.D. Elvira, Y. Feng, J. Freeman, A. Gandrakota, Z. Gecse, L. Gray, D. Green, A. Grummer, S. Grünendahl, D. Guerrero, O. Gutsche, R.M. Harris, R. Heller, T.C. Herwig, J. Hirschauer, B. Jayatilaka, S. Jindariani, M. Johnson, U. Joshi, T. Klijnsma, B. Klima, K.H.M. Kwok, S. Lammel, D. Lincoln, R. Lipton, T. Liu, C. Madrid, K. Maeshima, C. Mantilla, D. Mason, P. McBride, P. Merkel, S. Mrenna, S. Nahn, J. Ngadiuba, D. Noonan, S. Norberg, V. Papadimitriou, N. Pastika,

K. Pedro, C. Pena[86], F. Ravera, A. Reinsvold Hall[87], L. Ristori, M. Safdari, E. Sexton-Kennedy, N. Smith, A. Soha, L. Spiegel, S. Stoynev, J. Strait, L. Taylor, S. Tkaczyk, N.V. Tran, L. Uplegger, E.W. Vaandering, I. Zoi

University of Florida, Gainesville, Florida, USA
C. Aruta, P. Avery, D. Bourilkov, P. Chang, V. Cherepanov, R.D. Field, C. Huh, E. Koenig, M. Kolosova, J. Konigsberg, A. Korytov, K. Matchev, N. Menendez, G. Mitselmakher, K. Mohrman, A. Muthirakalayil Madhu, N. Rawal, S. Rosenzweig, Y. Takahashi, J. Wang

Florida State University, Tallahassee, Florida, USA
T. Adams, A. Al Kadhim, A. Askew, S. Bower, V. Hagopian, R. Hashmi, R.S. Kim, S. Kim, T. Kolberg, G. Martinez, H. Prosper, P.R. Prova, M. Wulansatiti, R. Yohay, J. Zhang

Florida Institute of Technology, Melbourne, Florida, USA
B. Alsufyani, M.M. Baarmand, S. Butalla, S. Das, T. Elkafrawy[19], M. Hohlmann, E. Yanes

University of Illinois Chicago, Chicago, Illinois, USA
M.R. Adams, A. Baty, C. Bennett, R. Cavanaugh, R. Escobar Franco, O. Evdokimov, C.E. Gerber, M. Hawksworth, A. Hingrajiya, D.J. Hofman, J.h. Lee, D. S. Lemos, A.H. Merrit, C. Mills, S. Nanda, G. Oh, B. Ozek, D. Pilipovic, R. Pradhan, E. Prifti, T. Roy, S. Rudrabhatla, N. Singh, M.B. Tonjes, N. Varelas, M.A. Wadud, Z. Ye, J. Yoo

The University of Iowa, Iowa City, Iowa, USA
M. Alhusseini, D. Blend, K. Dilsiz[88], L. Emediato, G. Karaman, O.K. Köseyan, J.-P. Merlo, A. Mestvirishvili[89], O. Neogi, H. Ogul[90], Y. Onel, A. Penzo, C. Snyder, E. Tiras[91]

Johns Hopkins University, Baltimore, Maryland, USA
B. Blumenfeld, L. Corcodilos, J. Davis, A.V. Gritsan, L. Kang, S. Kyriacou, P. Maksimovic, M. Roguljic, J. Roskes, S. Sekhar, M. Swartz

The University of Kansas, Lawrence, Kansas, USA
A. Abreu, L.F. Alcerro Alcerro, J. Anguiano, S. Arteaga Escatel, P. Baringer, A. Bean, Z. Flowers, D. Grove, J. King, G. Krintiras, M. Lazarovits, C. Le Mahieu, J. Marquez, M. Murray, M. Nickel, M. Pitt, S. Popescu[92], C. Rogan, C. Royon, R. Salvatico, S. Sanders, C. Smith, G. Wilson

Kansas State University, Manhattan, Kansas, USA
B. Allmond, R. Gujju Gurunadha, A. Ivanov, K. Kaadze, Y. Maravin, J. Natoli, D. Roy, G. Sorrentino

University of Maryland, College Park, Maryland, USA
A. Baden, A. Belloni, J. Bistany-riebman, Y.M. Chen, S.C. Eno, N.J. Hadley, S. Jabeen, R.G. Kellogg, T. Koeth, B. Kronheim, Y. Lai, S. Lascio, A.C. Mignerey, S. Nabili, C. Palmer, C. Papageorgakis, M.M. Paranjpe, E. Popova[93], A. Shevelev, L. Wang

Massachusetts Institute of Technology, Cambridge, Massachusetts, USA
J. Bendavid, I.A. Cali, P.c. Chou, M. D'Alfonso, J. Eysermans, C. Freer, G. Gomez-Ceballos, M. Goncharov, G. Grosso, P. Harris, D. Hoang, D. Kovalskyi,

J. Krupa, L. Lavezzo, Y.-J. Lee, K. Long, C. Mcginn, A. Novak, M.I. Park, C. Paus, C. Reissel, C. Roland, G. Roland, S. Rothman, G.S.F. Stephans, Z. Wang, B. Wyslouch, T. J. Yang

University of Minnesota, Minneapolis, Minnesota, USA
B. Crossman, B.M. Joshi, C. Kapsiak, M. Krohn, D. Mahon, J. Mans, B. Marzocchi, M. Revering, R. Rusack, R. Saradhy, N. Strobbe

University of Nebraska-Lincoln, Lincoln, Nebraska, USA
K. Bloom, D.R. Claes, G. Haza, J. Hossain, C. Joo, I. Kravchenko, J.E. Siado, W. Tabb, A. Vagnerini, A. Wightman, F. Yan, D. Yu

State University of New York at Buffalo, Buffalo, New York, USA
H. Bandyopadhyay, L. Hay, H.w. Hsia, I. Iashvili, A. Kalogeropoulos, A. Kharchilava, M. Morris, D. Nguyen, J. Pekkanen, S. Rappoccio, H. Rejeb Sfar, A. Williams, P. Young

Northeastern University, Boston, Massachusetts, USA
G. Alverson, E. Barberis, J. Bonilla, M. Campana, J. Dervan, Y. Haddad, Y. Han, A. Krishna, J. Li, M. Lu, G. Madigan, R. Mccarthy, D.M. Morse, V. Nguyen, T. Orimoto, A. Parker, L. Skinnari, D. Wood

Northwestern University, Evanston, Illinois, USA
J. Bueghly, S. Dittmer, K.A. Hahn, Y. Liu, Y. Miao, D.G. Monk, M.H. Schmitt, A. Taliercio, M. Velasco

University of Notre Dame, Notre Dame, Indiana, USA
G. Agarwal, R. Band, R. Bucci, S. Castells, A. Das, R. Goldouzian, M. Hildreth, K.W. Ho, K. Hurtado Anampa, T. Ivanov, C. Jessop, K. Lannon, J. Lawrence, N. Loukas, L. Lutton, J. Mariano, N. Marinelli, I. Mcalister, T. McCauley, C. Mcgrady, C. Moore, Y. Musienko[16], H. Nelson, M. Osherson, A. Piccinelli, R. Ruchti, A. Townsend, Y. Wan, M. Wayne, H. Yockey, M. Zarucki, L. Zygala

The Ohio State University, Columbus, Ohio, USA
A. Basnet, B. Bylsma, M. Carrigan, L.S. Durkin, C. Hill, M. Joyce, M. Nunez Ornelas, K. Wei, B.L. Winer, B. R. Yates

Princeton University, Princeton, New Jersey, USA
H. Bouchamaoui, K. Coldham, P. Das, G. Dezoort, P. Elmer, A. Frankenthal, B. Greenberg, N. Haubrich, K. Kennedy, G. Kopp, S. Kwan, D. Lange, A. Loeliger, D. Marlow, I. Ojalvo, J. Olsen, D. Stickland, C. Tully

University of Puerto Rico, Mayaguez, Puerto Rico, USA
S. Malik

Purdue University, West Lafayette, Indiana, USA
A.S. Bakshi, S. Chandra, R. Chawla, A. Gu, L. Gutay, M. Jones, A.W. Jung, A.M. Koshy, M. Liu, G. Negro, N. Neumeister, G. Paspalaki, S. Piperov, V. Scheurer, J.F. Schulte, M. Stojanovic, J. Thieman, A. K. Virdi, F. Wang, A. Wildridge, W. Xie, Y. Yao

Purdue University Northwest, Hammond, Indiana, USA
J. Dolen, N. Parashar, A. Pathak

Rice University, Houston, Texas, USA

D. Acosta, T. Carnahan, K.M. Ecklund, P.J. Fernández Manteca, S. Freed, P. Gardner, F.J.M. Geurts, I. Krommydas, W. Li, J. Lin, O. Miguel Colin, B.P. Padley, R. Redjimi, J. Rotter, E. Yigitbasi, Y. Zhang

University of Rochester, Rochester, New York, USA
A. Bodek, P. de Barbaro, R. Demina, J.L. Dulemba, A. Garcia-Bellido, O. Hindrichs, A. Khukhunaishvili, N. Parmar, P. Parygin[93], R. Taus

Rutgers, The State University of New Jersey, Piscataway, New Jersey, USA
B. Chiarito, J.P. Chou, S.V. Clark, D. Gadkari, Y. Gershtein, E. Halkiadakis, M. Heindl, C. Houghton, D. Jaroslawski, S. Konstantinou, I. Laflotte, A. Lath, R. Montalvo, K. Nash, J. Reichert, H. Routray, P. Saha, S. Salur, S. Schnetzer, S. Somalwar, R. Stone, S.A. Thayil, S. Thomas, J. Vora, H. Wang

University of Tennessee, Knoxville, Tennessee, USA
D. Ally, A.G. Delannoy, S. Fiorendi, S. Higginbotham, T. Holmes, A.R. Kanuganti, N. Karunarathna, L. Lee, E. Nibigira, S. Spanier

Texas A&M University, College Station, Texas, USA
D. Aebi, M. Ahmad, T. Akhter, O. Bouhali[94], R. Eusebi, J. Gilmore, T. Huang, T. Kamon[95], H. Kim, S. Luo, R. Mueller, D. Overton, D. Rathjens, A. Safonov

Texas Tech University, Lubbock, Texas, USA
N. Akchurin, J. Damgov, N. Gogate, V. Hegde, A. Hussain, Y. Kazhykarim, K. Lamichhane, S.W. Lee, A. Mankel, T. Peltola, I. Volobouev

Vanderbilt University, Nashville, Tennessee, USA
E. Appelt, Y. Chen, S. Greene, A. Gurrola, W. Johns, R. Kunnawalkam Elayavalli, A. Melo, F. Romeo, P. Sheldon, S. Tuo, J. Velkovska, J. Viinikainen

University of Virginia, Charlottesville, Virginia, USA
B. Cardwell, H. Chung, B. Cox, J. Hakala, R. Hirosky, A. Ledovskoy, C. Neu

Wayne State University, Detroit, Michigan, USA
S. Bhattacharya, P.E. Karchin

University of Wisconsin - Madison, Madison, Wisconsin, USA
A. Aravind, S. Banerjee, K. Black, T. Bose, S. Dasu, I. De Bruyn, P. Everaerts, C. Galloni, H. He, M. Herndon, A. Herve, C.K. Koraka, A. Lanaro, R. Loveless, J. Madhusudanan Sreekala, A. Mallampalli, A. Mohammadi, S. Mondal, G. Parida, L. Pétré, D. Pinna, A. Savin, V. Shang, V. Sharma, W.H. Smith, D. Teague, H.F. Tsoi, W. Vetens, A. Warden

Authors affiliated with an institute or an international laboratory covered by a cooperation agreement with CERN
S. Afanasiev, V. Alexakhin, D. Budkouski, I. Golutvin†, I. Gorbunov, V. Karjavine, V. Korenkov, A. Lanev, A. Malakhov, V. Matveev[96], V. Palichik, V. Perelygin, M. Savina, V. Shalaev, S. Shmatov, S. Shulha, V. Smirnov, O. Teryaev, N. Voytishin, B.S. Yuldashev[97], A. Zarubin, I. Zhizhin, G. Gavrilov, V. Golovtcov, Y. Ivanov, V. Kim[96], P. Levchenko[98], V. Murzin, V. Oreshkin, D. Sosnov, V. Sulimov, L. Uvarov, A. Vorobyev†, Yu. Andreev, A. Dermenev, S. Gninenko, N. Golubev, A. Karneyeu, D. Kirpichnikov, M. Kirsanov, N. Krasnikov, I. Tlisova, A. Toropin, T. Aushev, V. Gavrilov, N. Lychkovskaya, A. Nikitenko[99,100], V. Popov, A. Zhokin, R. Chistov[96], M. Danilov[96],

S. Polikarpov[96], V. Andreev, M. Azarkin, M. Kirakosyan, A. Terkulov, E. Boos, V. Bunichev, M. Dubinin[86], L. Dudko, A. Ershov, A. Gribushin, V. Klyukhin, S. Obraztsov, M. Perfilov, V. Savrin, P. Volkov, G. Vorotnikov, V. Blinov[96], T. Dimova[96], A. Kozyrev[96], O. Radchenko[96], Y. Skovpen[96], V. Kachanov, D. Konstantinov, S. Slabospitskii, A. Uzunian, A. Babaev, V. Borshch, D. Druzhkin[101]

Authors affiliated with an institute formerly covered by a cooperation agreement with CERN
V. Chekhovsky, V. Makarenko

†: Deceased
[1]Also at Yerevan State University, Yerevan, Armenia
[2]Also at TU Wien, Vienna, Austria
[3]Also at Ghent University, Ghent, Belgium
[4]Also at Universidade do Estado do Rio de Janeiro, Rio de Janeiro, Brazil
[5]Also at Universidade Estadual de Campinas, Campinas, Brazil
[6]Also at Federal University of Rio Grande do Sul, Porto Alegre, Brazil
[7]Also at UFMS, Nova Andradina, Brazil
[8]Also at Nanjing Normal University, Nanjing, China
[9]Now at The University of Iowa, Iowa City, Iowa, USA
[10]Also at University of Chinese Academy of Sciences, Beijing, China
[11]Also at China Center of Advanced Science and Technology, Beijing, China
[12]Also at University of Chinese Academy of Sciences, Beijing, China
[13]Also at China Spallation Neutron Source, Guangdong, China
[14]Now at Henan Normal University, Xinxiang, China
[15]Also at Université Libre de Bruxelles, Bruxelles, Belgium
[16]Also at an institute or an international laboratory covered by a cooperation agreement with CERN
[17]Also at Zewail City of Science and Technology, Zewail, Egypt
[18]Also at British University in Egypt, Cairo, Egypt
[19]Now at Ain Shams University, Cairo, Egypt
[20]Also at Purdue University, West Lafayette, Indiana, USA
[21]Also at Université de Haute Alsace, Mulhouse, France
[22]Also at Istinye University, Istanbul, Turkey
[23]Also at Ilia State University, Tbilisi, Georgia
[24]Also at The University of the State of Amazonas, Manaus, Brazil
[25]Also at University of Hamburg, Hamburg, Germany
[26]Also at RWTH Aachen University, III. Physikalisches Institut A, Aachen, Germany
[27]Also at Bergische University Wuppertal (BUW), Wuppertal, Germany
[28]Also at Brandenburg University of Technology, Cottbus, Germany
[29]Also at Forschungszentrum Jülich, Juelich, Germany
[30]Also at CERN, European Organization for Nuclear Research, Geneva, Switzerland
[31]Also at HUN-REN ATOMKI - Institute of Nuclear Research, Debrecen, Hungary
[32]Now at Universitatea Babes-Bolyai - Facultatea de Fizica, Cluj-Napoca, Romania
[33]Also at MTA-ELTE Lendület CMS Particle and Nuclear Physics Group, Eötvös Loránd University, Budapest, Hungary
[34]Also at HUN-REN Wigner Research Centre for Physics, Budapest, Hungary
[35]Also at Physics Department, Faculty of Science, Assiut University, Assiut, Egypt
[36]Also at Punjab Agricultural University, Ludhiana, India
[37]Also at University of Visva-Bharati, Santiniketan, India
[38]Also at Indian Institute of Science (IISc), Bangalore, India

[39]Also at IIT Bhubaneswar, Bhubaneswar, India
[40]Also at Institute of Physics, Bhubaneswar, India
[41]Also at University of Hyderabad, Hyderabad, India
[42]Also at Deutsches Elektronen-Synchrotron, Hamburg, Germany
[43]Also at Isfahan University of Technology, Isfahan, Iran
[44]Also at Sharif University of Technology, Tehran, Iran
[45]Also at Department of Physics, University of Science and Technology of Mazandaran, Behshahr, Iran
[46]Also at Department of Physics, Isfahan University of Technology, Isfahan, Iran
[47]Also at Department of Physics, Faculty of Science, Arak University, ARAK, Iran
[48]Also at Helwan University, Cairo, Egypt
[49]Also at Italian National Agency for New Technologies, Energy and Sustainable Economic Development, Bologna, Italy
[50]Also at Centro Siciliano di Fisica Nucleare e di Struttura Della Materia, Catania, Italy
[51]Also at Università degli Studi Guglielmo Marconi, Roma, Italy
[52]Also at Scuola Superiore Meridionale, Università di Napoli 'Federico II', Napoli, Italy
[53]Also at Fermi National Accelerator Laboratory, Batavia, Illinois, USA
[54]Also at Consiglio Nazionale delle Ricerche - Istituto Officina dei Materiali, Perugia, Italy
[55]Also at Department of Applied Physics, Faculty of Science and Technology, Universiti Kebangsaan Malaysia, Bangi, Malaysia
[56]Also at Consejo Nacional de Ciencia y Tecnología, Mexico City, Mexico
[57]Also at Trincomalee Campus, Eastern University, Sri Lanka, Nilaveli, Sri Lanka
[58]Also at Saegis Campus, Nugegoda, Sri Lanka
[59]Also at National and Kapodistrian University of Athens, Athens, Greece
[60]Also at Ecole Polytechnique Fédérale Lausanne, Lausanne, Switzerland
[61]Also at University of Vienna, Vienna, Austria
[62]Also at Universität Zürich, Zurich, Switzerland
[63]Also at Stefan Meyer Institute for Subatomic Physics, Vienna, Austria
[64]Also at Laboratoire d'Annecy-le-Vieux de Physique des Particules, IN2P3-CNRS, Annecy-le-Vieux, France
[65]Also at Near East University, Research Center of Experimental Health Science, Mersin, Turkey
[66]Also at Konya Technical University, Konya, Turkey
[67]Also at Izmir Bakircay University, Izmir, Turkey
[68]Also at Adiyaman University, Adiyaman, Turkey
[69]Also at Bozok Universitetesi Rektörlügü, Yozgat, Turkey
[70]Also at Marmara University, Istanbul, Turkey
[71]Also at Milli Savunma University, Istanbul, Turkey
[72]Also at Kafkas University, Kars, Turkey
[73]Now at Istanbul Okan University, Istanbul, Turkey
[74]Also at Hacettepe University, Ankara, Turkey
[75]Also at Erzincan Binali Yildirim University, Erzincan, Turkey
[76]Also at Istanbul University - Cerrahpasa, Faculty of Engineering, Istanbul, Turkey
[77]Also at Yildiz Technical University, Istanbul, Turkey
[78]Also at Vrije Universiteit Brussel, Brussel, Belgium
[79]Also at School of Physics and Astronomy, University of Southampton, Southampton, United Kingdom
[80]Also at IPPP Durham University, Durham, United Kingdom
[81]Also at Monash University, Faculty of Science, Clayton, Australia

[82]Also at Institute of Basic and Applied Sciences, Faculty of Engineering, Arab Academy for Science, Technology and Maritime Transport, Alexandria, Egypt
[83]Also at Università di Torino, Torino, Italy
[84]Also at Bethel University, St. Paul, Minnesota, USA
[85]Also at Karamanoğlu Mehmetbey University, Karaman, Turkey
[86]Also at California Institute of Technology, Pasadena, California, USA
[87]Also at United States Naval Academy, Annapolis, Maryland, USA
[88]Also at Bingol University, Bingol, Turkey
[89]Also at Georgian Technical University, Tbilisi, Georgia
[90]Also at Sinop University, Sinop, Turkey
[91]Also at Erciyes University, Kayseri, Turkey
[92]Also at Horia Hulubei National Institute of Physics and Nuclear Engineering (IFIN-HH), Bucharest, Romania
[93]Now at another institute or international laboratory covered by a cooperation agreement with CERN
[94]Also at Texas A&M University at Qatar, Doha, Qatar
[95]Also at Kyungpook National University, Daegu, Korea
[96]Also at another institute or international laboratory covered by a cooperation agreement with CERN
[97]Also at Institute of Nuclear Physics of the Uzbekistan Academy of Sciences, Tashkent, Uzbekistan
[98]Also at Northeastern University, Boston, Massachusetts, USA
[99]Also at Imperial College, London, United Kingdom
[100]Now at Yerevan Physics Institute, Yerevan, Armenia
[101]Also at Universiteit Antwerpen, Antwerpen, Belgium